博士論文

Modelling of Geothermal Well Cuttings Transportation during Drilling: A Case Study of Well PW-03B in Paka Geothermal Field, Kenya

地熱井掘削時の掘屑運搬のモデル化：ケニア共和国パカ地熱フィールド PW-03B 坑井におけるケーススタディ

Thomas Miyora Ong'au
トーマス・ミヨラ・オンガウ

Modelling of Geothermal Well Cuttings Transportation during Drilling, A Case Study of Well PW-03B in Paka Geothermal Field, Kenya

by

Thomas Miyora Ong'au

Presented to

Graduate School of International Resource Sciences

Akita University

for the Degree of

Doctor of Philosophy

in the field of Earth Resource Engineering and Environmental Sciences

March 2024

Abstract

The cost of a geothermal well depends heavily on the drilling time and it is crucial to minimize downtime during drilling. For geothermal wells drilled within the North Rift, Kenya, experience has shown that a higher rate of penetration (ROP) can be achieved, for example, by using polycrystalline diamond compact (PDC) drill bits instead of roller cone bits. However, operators have been hesitant to drill at high ROPs since such operation settings have been associated with an increased occurrence of stuck pipe situations. Increasing the ROP requires removing drill cuttings more effectively and at a higher rate to avoid accumulations of cuttings in the well. Firstly, accumulation of cuttings in the well annulus may result in direct mechanical sticking of the drill string. Secondly, it may also cause increased equivalent circulating density (ECD) leading to fracturing and wall collapse that can cause drill string sticking. Therefore, insufficient transport and removal of drill cuttings increases the risk of stuck pipe.

This study looked at determining optimum hole cleaning parameters for drilling geothermal wells in the North Rift geothermal fields in Kenya. The goal was to establish what drilling parameter settings are needed to enable safe drilling at the high ROPs that have been shown to be achievable. This work explores optimal hole-cleaning parameters based on numerical simulations that are supported by field observations. A Transient-Cuttings-Transport (TCT) simulator developed by Uematsu (2003), and Naganawa and Nomura (2006) was modified to model cuttings transport for a well drilled in Paka geothermal field, Kenya. The simulations describing a moderately inclined well account for the cuttings concentration and loss of circulation zones. Drilling fluid consisting of aerated water was considered in the simulations.

Optimal combinations of water and air flow rates were estimated for effective hole cleaning to achieve optimal ROPs. The model was validated using field data from the Paka geothermal field in Kenya. Optimal drilling parameters are recommended for actual field application to effectively reduce the current drilling time.

Acknowledgement

I wish to thank God for enabling and sustaining me throughout my study period in Japan and more specifically in Akita University

I wish to thank the Japanese government through JICA and Geothermal Development Company Limited who financially made the study possible.

I wish to specially thank my supervisors Prof Shigemi Naganawa and Dr Elvar Bjarkason who guided me in my studies and research work.

I wish to thank the staff in the Faculty of International Resource Sciences, including Ms Kurabe and Ms Horino who have been of great help to me in administration work. I also wish to thank the Geosystems Engineering Lab fellows at Akita University for their support and encouragement.

Finally, special gratitude to my family: my dear Wife Evah, my daughters Monicah and Jedidah and son Peter who had to endure my absence and moreover gave me the moral support to endure the separation while undertaking the study.

Table of Contents

List of Tables

List of Figures

Chapter 1
Introduction

1.1 Background

Drilling for oil, gas, or geothermal is an expensive undertaking that is time dependent. The ideal scenario is to drill a well in the shortest time possible to the target depth and start well completions. This is not always the case since every well has unforeseen downhole challenges. According to Azar and Samuel (2007), some form of drilling problem will most certainly occur even after putting careful drilling plans in place. Therefore, the key to succeed in effective drilling is to plan drilling of wells in anticipation of these problems. Azar and Samuel stated the most common drilling problems as follows:

- Stuck pipes
- Lost circulation
- Hole deviation
- Pipe failure
- Borehole instability
- Mud contamination
- Formation damage
- Hole cleaning
- H_2S-bearing formations
- Equipment and personnel related problems.

Each of the problems stated above can be dealt with according to drilling engineering practices and experiences that have been tried in different fields under different conditions. Careful analysis of these problems shows that most of them are closely related to hole cleaning. Hole cleaning encompasses other aspects such as drilling fluid properties, drilling fluid velocity, geometric characteristics of the well, cuttings characteristics, rate of penetration and annulus/pipe eccentricity. Stuck pipe may either be differential or mechanical and is closely related to hole cleaning. Improper hole cleaning in deviated holes will lead to drilling problems.

Borehole instability, mud contamination, formation damage and lost circulation may be linked to hole cleaning and drilling fluids design which in turn lead to stuck pipe (Lyons and Plisga, 2005).

The observations above show that hole cleaning during drilling is vital and is a condition that has to be met for successful drilling to occur. Hole cleaning basically refers to evacuation of cuttings; generated by the bit and from the side of the well; from the well to the surface using drilling fluids.

1.2 Objectives of the Research

In recognition that these problems have a big impact on the time taken to drill a well and by extension the overall cost of the well, designing effective cuttings transportation parameters is imperative in alleviating the problems (Azar and Samuel, 2007).

The research interest of this study is in the area of cuttings transportation from the hole to the surface for geothermal wells. Consequently, other factors that affect cuttings transportation to the surface will also be studied such as the drilling fluid used. The fluid characteristics have to be taken into account since they are the ones that carry the cuttings to the surface. Other peripheral factors such as lost circulation zones, hole geometry and size, will also be investigated in order to determine the most optimum way to transport cuttings to the surface.

This study looks at modelling of hole cleaning parameters for wells drilled within the Paka geothermal field in Kenya. The model will be used to obtain optimal hole cleaning conditions through analysing drilling performance data from a well recently drilled in the Paka field.

1.3 Basics of Drilling Operations Process

Drilling for oil, gas, or geothermal is done using a drilling rig set up on a drilling platform on land or sea. After the drilling rig has been set up, drilling a well involves following up a systematic set of events which will culminate in a complete well. Rotary drilling rigs are used for almost all drilling today as summarized in Figure 1. The hole is drilled by rotating the drill bit on the bottom of the hole with weight provided by the bottom hole assembly of the drilling string. The cuttings of the formation rock generated by the bit are transported to the surface by

circulating a drilling fluid down the drilling string through the drill bit and up through the wellbore annulus to the surface. The cuttings are then separated from the drilling fluid on the surface and the drilling fluid is recirculated back for further drilling. (Bourgoyne et al.,1991).

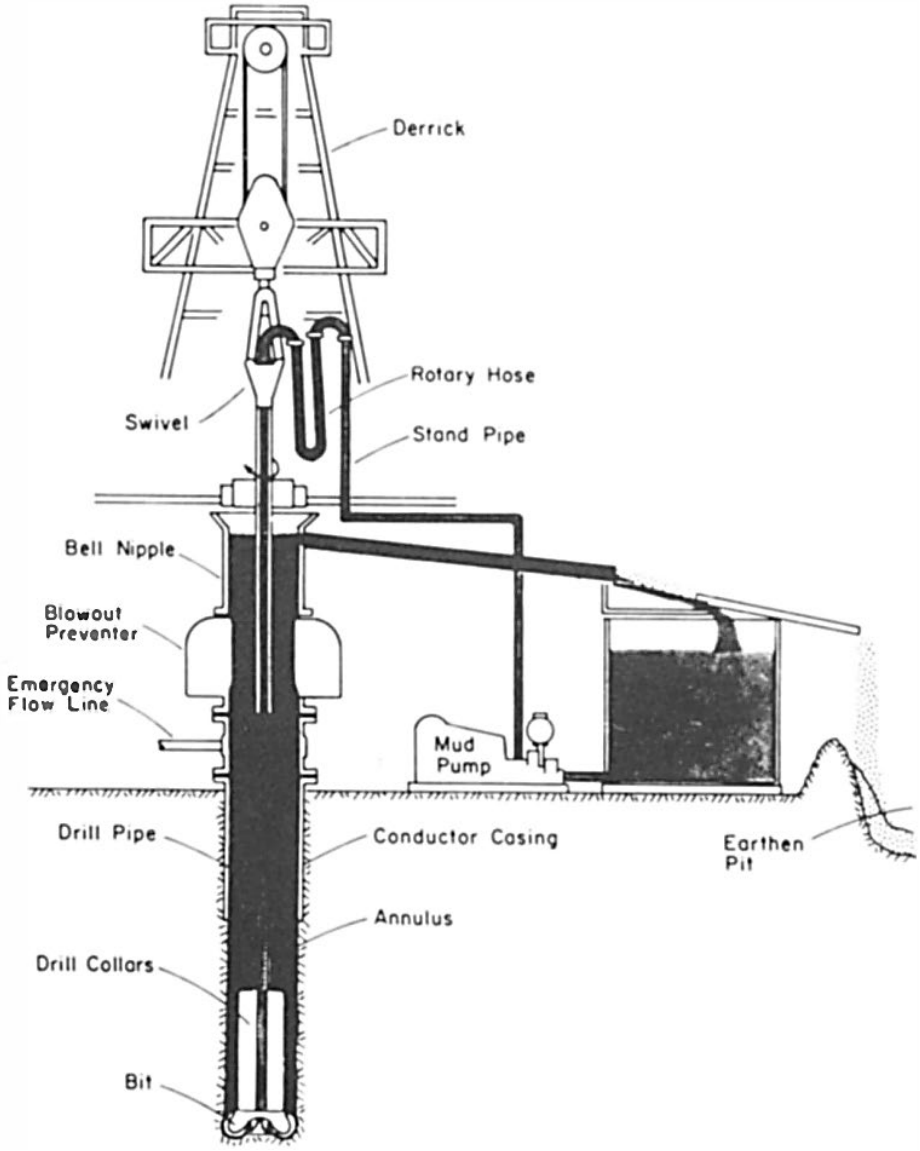

Figure 1: Rotary drilling process (Bourgoyne et al., 1991).

1.3.1 Drilling Rig Systems

The drilling rig is made up several different components. Each component has unique functions that makes rig operational. Ford (2004) identifies six systems that make up a rotary drilling rig as:

- Power system
- Hoisting system

- Circulation system
- Rotary system
- Well control system
- Monitoring system (Drilling data acquisition).

The systems stated are found both in land and offshore rigs.

1.3.2 The Circulation System

The circulating system is used to circulate the drilling fluid down the drilling string, to the drill bit where the cuttings are generated, and up the annulus carrying the cuttings with it to the surface (Ford, 2004). The circulating system consists of the following (Guo and Liu et al., 2011):

- Mud tanks and pit
- Mud pumps
- Standpipe, kelly and drill string
- Drill bit
- Return annulus
- Contaminant removal equipment: Shale shakers, degassers, hydro-cyclones and centrifuges

When using aerated drilling fluids, additional equipment used includes:

- Air compressors
- Rotating head
- Blooey line

The drilling fluids used can be mud, water, air, aerated mud, aerated water or aerated water and foam. In Paka geothermal field, aerated water and foam is used as the drilling fluid. Concurrently, the following fluids are pumped through the standpipe: water from the mud tanks is pumped by triplex mud pumps, air from the compressors is also pumped and finally, drilling detergent is pumped by a dosing pump. All three fluid components are then pumped down the drilling string as a mixture of aerated water and foam. The drilling fluid then comes out the drill bit and up the annulus carrying with cuttings.

At the surface, there is a rotating head that makes it possible for the aerated water and foam to be directed to the shale shakers through the mud line return. Returned air, water and the

cuttings are separated there where the cuttings and air are discarded and the water is circulated back to the mud tanks. Figure 2 shows a typical circulating system for water or mud drilling, and Figure 3 shows a typical circulating system for aerated drilling.

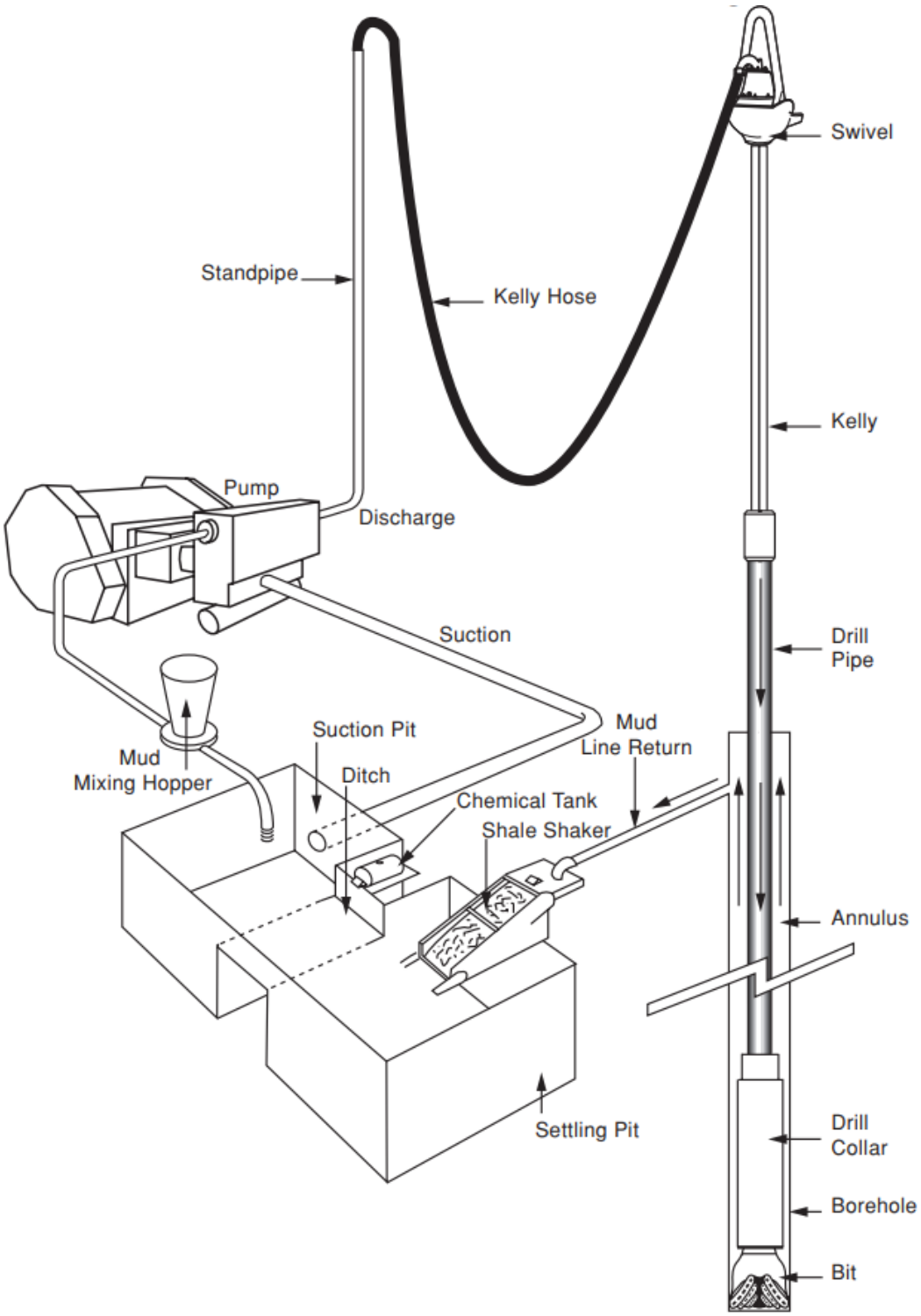

Figure 2: Typical circulating system (Ford, 2004).

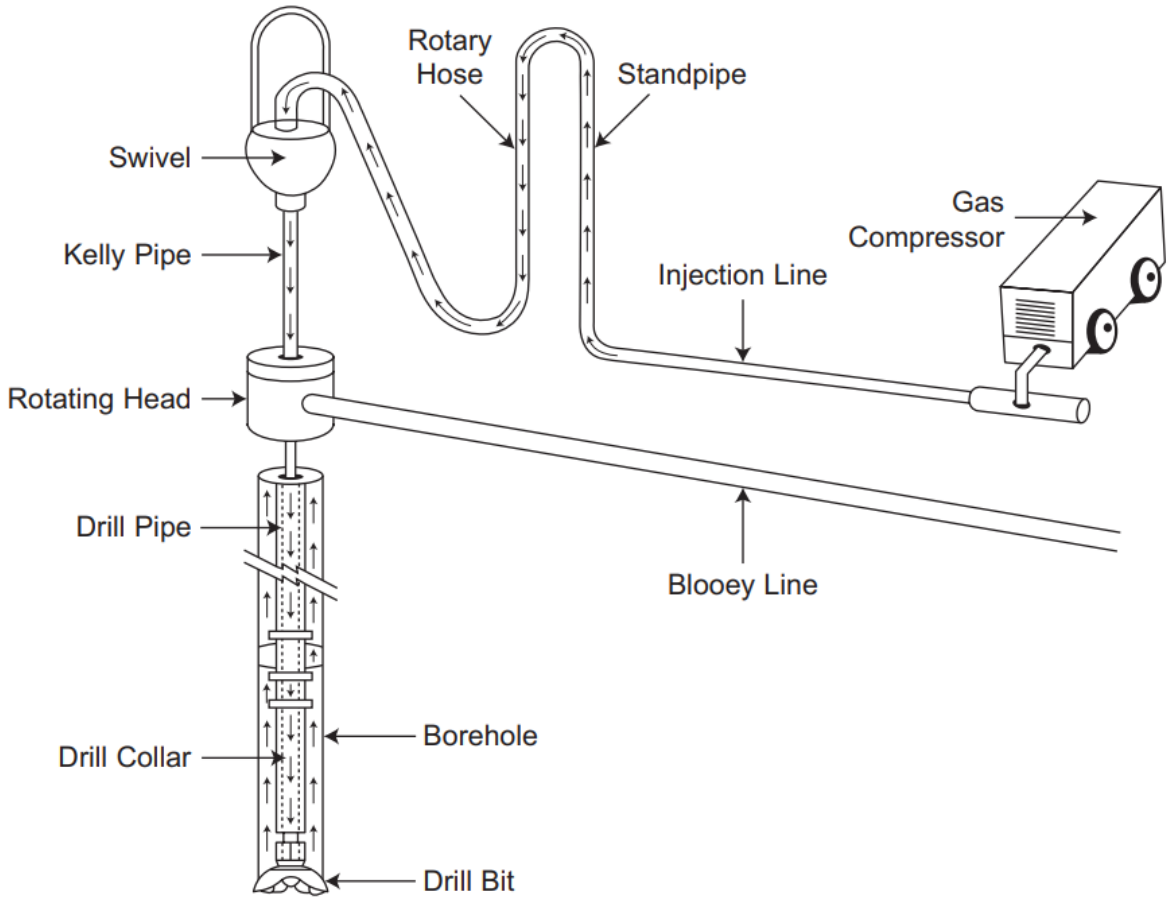

Figure 3: Typical circulation system with aerated drilling equipment (Ford, 2004).

1.4 Differences Between Oil Drilling and Geothermal Drilling

Drilling both in the oil industry and geothermal industry basically utilizes the same type of equipment, which is a drilling rig. However, there are major differences when it comes to drilling in either of these fields as highlighted in Table 1.

Table 1: Difference between geothermal and oil drilling.

Geothermal Drilling	Oil Drilling
High temperatures during drilling are encountered and bottom hole circulation temperature may be over 100°C	Relative low bottom hole circulation temperatures during drilling.
The rock types are mostly volcanic and they are hard and abrasive with low ROP	The rocks are mostly sedimentary and they are soft with high ROP
The geothermal formation is highly fractured with loss of circulation and drilling long sections without returns is very common	Loss of circulation is not common and healing loss zones is priority.
Cementing of the casings is usually back to the surface except for the slotted liner casings which are not cemented	Not all casings are cemented back to the surface.
Well control is mostly by filling the well bore with drilling fluid and also using BOP equipment.	Well control is by use of drilling fluid density BOP. Well design is critical in oil wells to avoid blowout.

1.5 Problem Statement and Research Questions

From the study of time analysis during drilling of geothermal wells, 20% or more of the total drilling time is taken up by non-productive time (NPT). 50% or more of the NPT time is a result of downhole problems (Ong'au, 2010; Okwiri, 2015; Saleh et al., 2020). Most of the downhole problems are related to drilling fluid design and hole cleaning. Understanding and developing a thorough hole cleaning program is crucial for successful drilling.

This research assesses the cuttings transport process and designs optimum parameters to be used for cleaning geothermal wells to minimize downhole problems as a result of cuttings accumulation in the annulus. Factors that closely affect cuttings transportation are examined and a relationship established here for a model to efficiently transport cuttings from the hole will pave the way for efficient and safe drilling operations. Drilling data for geothermal wells in Paka geothermal field in Baringo County, Kenya were used for the model development. Since most of the challenges are experienced when drilling the production section of wells from 300 m downwards, the research concentrates on sections below 300 m. Mostly aerated water and foam is used as the drilling fluid in these sections.

In this research following questions will be addressed:

1. How different are the cuttings transport behaviors between using water only and using aerated water?
2. What is the effect of loss of circulation on cuttings transport?
3. What are the cuttings bed characteristics for the Paka well under study?
4. Can an effective cuttings transport be modelled for geothermal well drilling and then be optimized to effectively improve rate of penetration (ROP)?

Chapter 2
Literature Review

2.1 Related Studies Done

Cuttings transport is a research area that has elicited many research studies for both vertical and directional wells.

Bourgoyne et al. (1991) stated that adequate cuttings transport can be achieved when we have large enough pressure pumps, large diameter drill pipes and low viscosity drilling fluid. Adequate hole cleaning can be achieved by either maximizing jet impact or maximizing hydraulic horsepower. Bourgoyne et al. proposed the approach of maximising ROP and minimizing cost and hence dictating parameters for cuttings transportation. According to Bourgoyne et al., the variables that help achieve hole cleaning during drilling are slip velocity, annular velocity and cuttings transport velocity which is the difference between annular velocity and slip velocity. For positive transport velocity, the cuttings will be transported to the surface.

Bourgoyne et al. also stated that the three most approved correlations for determining slip velocity are the Chien (1969), Moore (1974), and Walker and Mayes (1976) correlations. Sample and Bourgoyne (1978) also came up with a method of determining slip velocity by plotting transport velocity versus the inverse of annular velocity. The *y*-intercept of this plot corresponds to the inverse of slip velocity. From the statistical analysis of field data using Chien correlation, Moore correlation, Walker and Mayes correlation, and Sample and Bourgoyne method, however, it can be recommended that the most accurate correlation for determining slip velocity to be the Moore correlation. Bourgoyne et al. (1991) observed that a high cuttings concentration in the annuli causes high effective mud density which leads to high a circulating bottom hole pressure and hence a low ROP.

Azar and Samuel (2007) stated that if cuttings are not removed immediately from the bottom of the hole, they cause retard drilling and bit wear. They also increase the effective mud weight in the well which can cause fracturing of the well and reduce penetration rate.

For vertical wells, Azar and Samuel pointed out that the three important variables that influence hole cleaning are the average cuttings slip velocity, average cuttings transport velocity, and average annular volumetric cuttings concentration. He presented three most preferred correlations for determining the slip velocity; Chien, Moore, and Walker and Mayes correlations. From the slip velocity, the average cuttings transport velocity is determined. The average cuttings concentration is determined from statistics of field data experience and Azar and Samuel gave 5% as the highest cuttings concentration by volume in the annulus for trouble free drilling.

For inclined and horizontal wells, Azar and Samuel pointed out that the cuttings transportation becomes complex because of the formation of cuttings beds, eccentric flow regimes and variable impact of gravity. Inclined wells are classified into categories. First, wells with inclination angles of 0-10° have adequate and reliable solutions for cuttings transportation. For wells with inclination greater than 10°, the inclined well and the eccentricity nature of pipe rotation poses a challenge in getting adequate solutions. Wells with inclination angles of 10-20° and annular velocities of less than 120 ft/min (= 0.61 m/s) results in formation of cuttings beddings. For holes with inclination angles of more than 35°, the critical velocity must be determined below which cuttings cannot be adequately cleaned. From field data, the critical velocity is the annular velocity which ensure that the cuttings concentration in the annulus are less than 5% by volume. Holes with inclination angles of more than 40° have the critical velocity that will ensure that no cuttings beddings forms within the annulus.

In his extensive research papers in cuttings transportation in oil wells, Naganawa et al. (2002) has looked at cuttings transportation in various conditions.

Naganawa (2013) reported results on cuttings transportation in highly inclined geothermal wells with inclination angles greater than 60°. This research was conducted on a large-scale flow loop apparatus known as Cuttings Transport Flow Loop System (CTFLS). Optimum fluid parameters (type of fluid, density, viscosity, yield point and gel strength) and operation parameters (rotational speed of drill pipe and ROP) were determined and proposed for use in getting optimum cuttings transportation for highly inclined geothermal wells. The optimum

fluid flow rate when using water was recommended as 0.53 m/s where there is a minimum frictional pressure loss and the cuttings concentration reasonably low. When using mud with a specific gravity of 1.03, the flow rate was recommended to be 0.63 m/s. The study showed that in drilling highly inclined geothermal wells, excessive fluid flow rate is not preferable in order to prevent increase in frictional pressure loss. The result of the study also recommended that the ROP must be controlled in order to control cuttings concentration in the annulus which in turn will control frictional pressure loss. It was also confirmed from the study that drill pipe rotation had the advantage of mechanically agitating cuttings hence promoting their transportation. In drilling geothermal wells, low-viscosity drilling fluid such as water may be an important option due to its ability to supress frictional pressure loss and reasonable cuttings transportation efficiency due to turbulence.

2.2 Geothermal Drilling in Kenya—Olkaria Field

Geothermal exploration in Kenya started in the 1960s and this resulted in the first two wells drilled in the Olkaria geothermal field in the 1970s. After extensive exploration and firming on drilling sites, exploration drilling and production drilling were carried out from 1973 to early 1980s. The first power plant of 15 MW was constructed and commissioned in June 1981 (Simiyu , 2010).

A detailed time analysis study of directional wells drilled in 2008 in Olkaria showed that the average time to drill a well to a depth of 2830 m was 57 days. The depth versus time drilling curves for some of the wells drilled in the Olkaria geothermal field are as shown in Figure 4 (Ong'au, 2012).

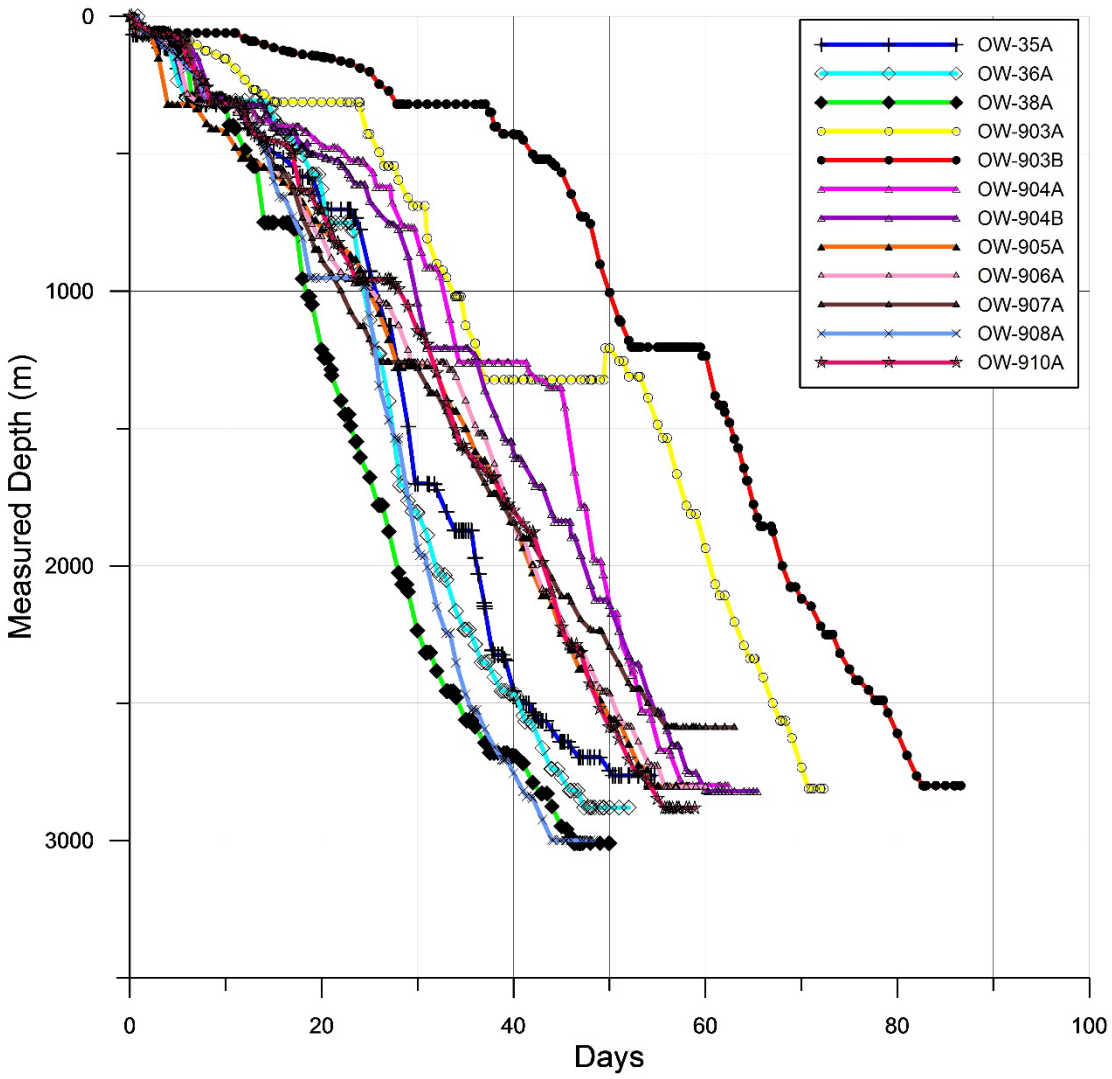

Figure 4: Depth versus days for wells drilled in Olkaria geothermal field (Ong'au, 2012).

2.3 Geothermal Drilling in Kenya—Menengai Field

Drilling in Menengai geothermal field started in February 2011 and over 50 high-temperature and high-pressure wells were drilled by the year 2020 when drilling temporarily stopped to pave way for power plant construction. Figure 5 shows the depth versus days for some wells drilled in the Menengai geothermal field. The average drilling time for Menengai wells was about 96 days and the average drilled depth was 1959 m (Okwiri, 2015).

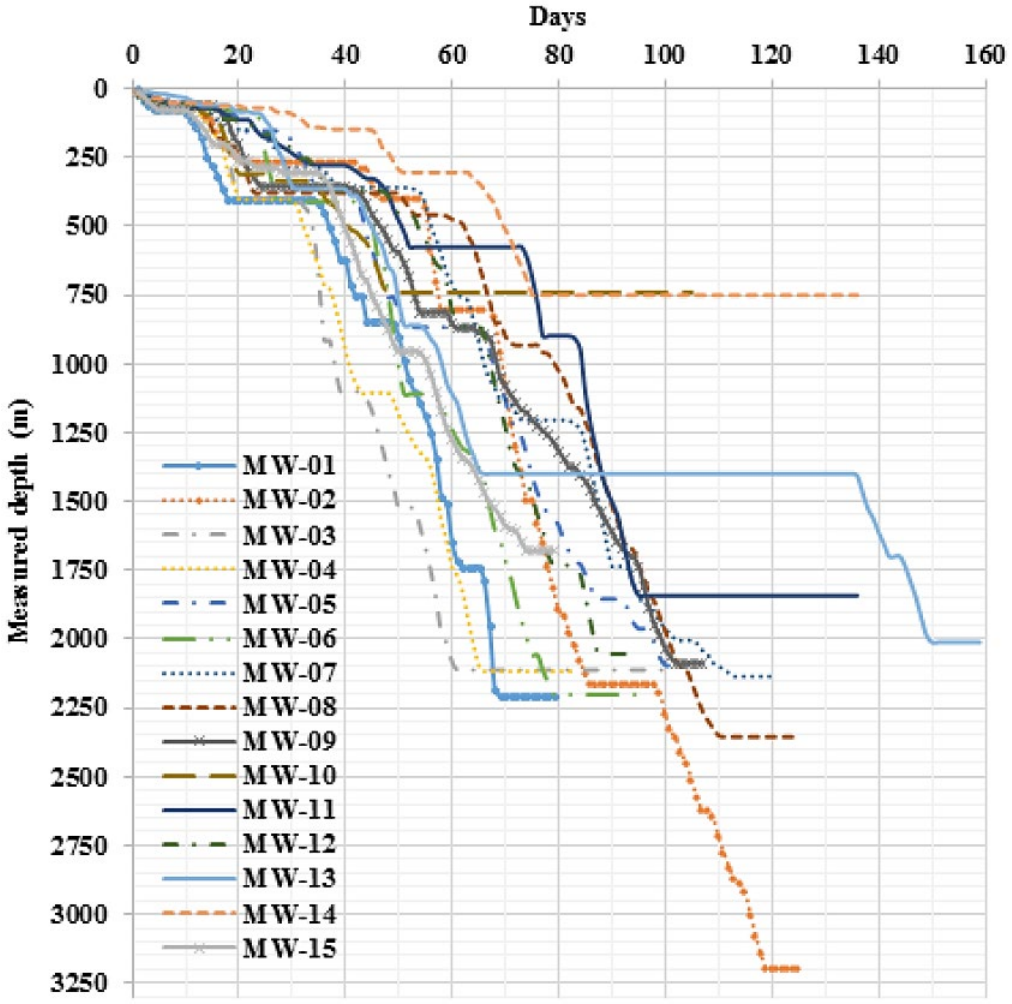

Figure 5: Depth versus days for wells drilled in Menengai geothermal field (Okwiri, 2015).

2.4 Geothermal Drilling in Kenya—Paka Geothermal Field

Paka geothermal field is one of the many geothermal fields found within the Kenyan Rift Valley, towards the Northern side. Exploration drilling in Paka started in December 2018 by drilling well PW-01. As of June 2023, 14 wells had been drilled in Paka geothermal field. Figure 6 shows the relative position of Paka geothermal field.

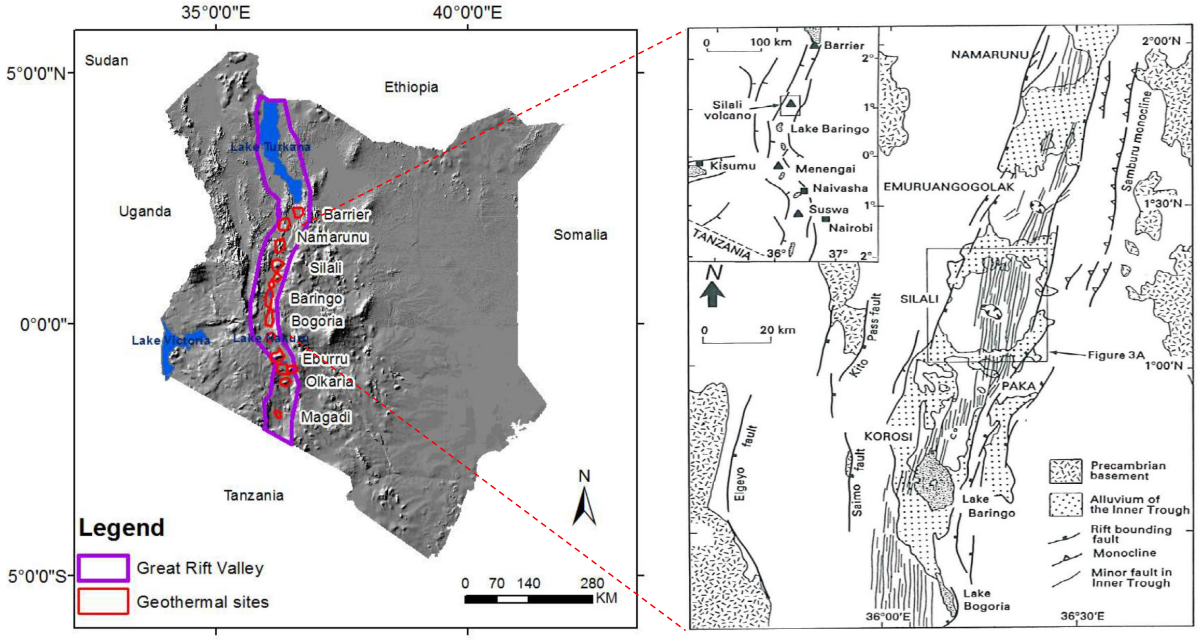

Figure 6: Locations of geothermal prospects in Kenya. The zoomed part shows the Korosi, Paka and Silali geothermal fields. Adapted from Macharia et al. (2017) and Mutonga (2012).

2.4.1 The Geology of Paka Geothermal Field

Paka geothermal field is located within the Kenyan Rift segment which is part of the East African Rift system. It is a shield volcanic complex. This volcanic complex is located within the Baringo-Silali geothermal block. It consists of trachytic and basaltic volcanic sequences that erupted in the last 390 ka. The Paka volcanic complex is approximately 136 km^2 in area. Exploration of Paka indicates that it has four volcanic sequences that are composed mainly of trachytic lava with intercalations of basalt and pyroclastic deposits. (Mibei et al., 2022). The faults within the volcano in Paka geothermal field mainly have a right stepping arrangement. The faults are both N-S and NNE-NE trending. The NE trending faults appear to have a greater influence in the underlying hydrothermal and magmatic systems (Mibei et al., 2021).

Paka field has many geothermal manifestations such as fumaroles, hot springs, altered hot grounds, steaming grounds, sulphur deposits, a high CO_2 gas concentration among others. The manifestations are mostly visible at the high grounds of the caldera area and towards the north but are scarce southwards. This is possibly because the manifestations have been buried by tuff deposits from the volcanic sequences (Mibei et al., 2021). Figure 7 shows a general geological map of Paka geothermal field.

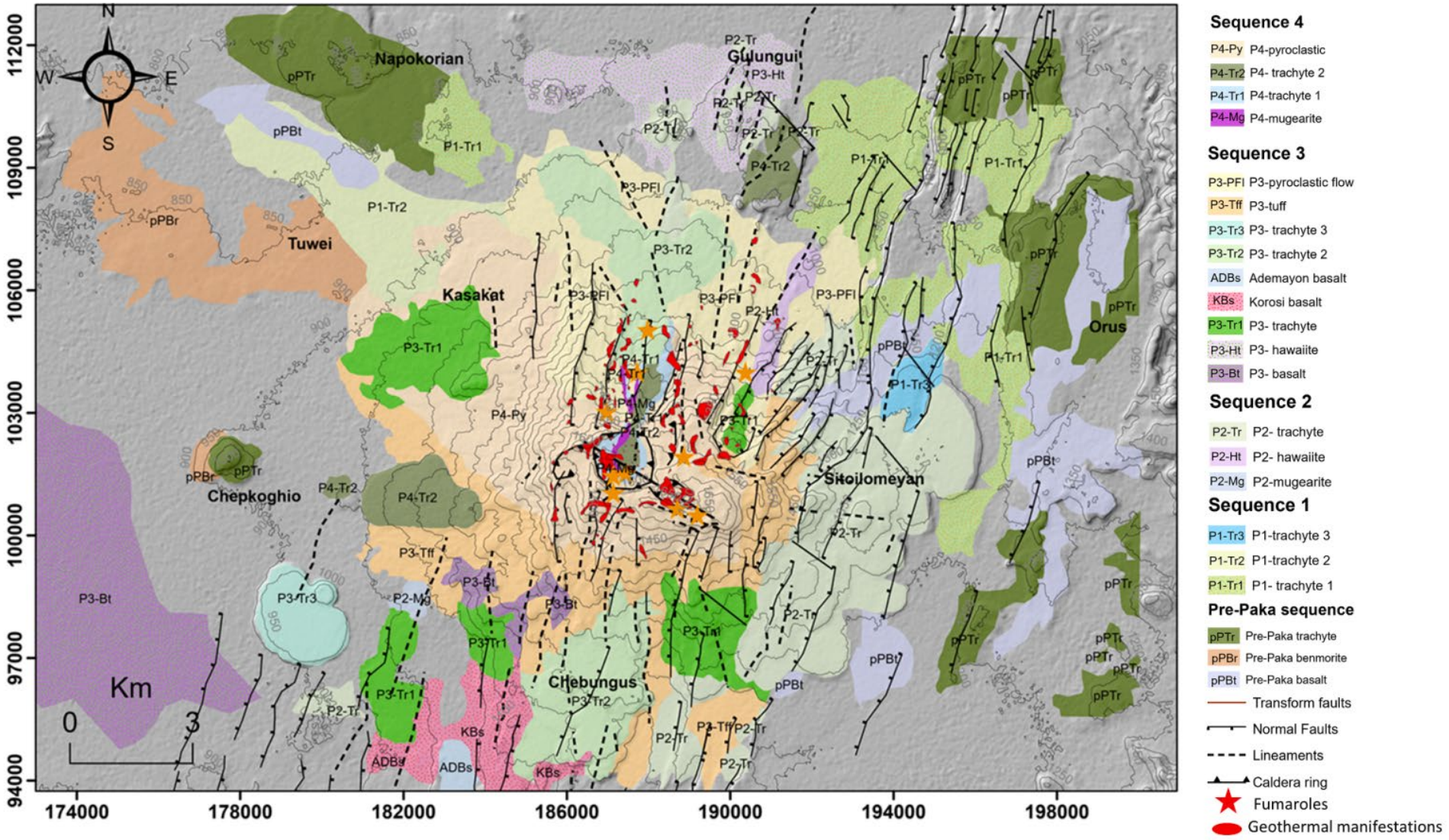

Figure 7: Geological map of Paka (Mibei et al., 2022).

2.4.2 Typical Well Design in Paka Geothermal Field

The Paka wells are designed to be drilled to a target measured depth of 3000 m. However, most of the wells drilled did not reach their target depth due to downhole drilling challenges of high torque and drag. Although formation factors may have resulted in these drilling challenges, insufficient hole cleaning and cuttings transportation is suspected to be one of the main causes. Table 2 shows a typical well design for wells drilled within the Paka geothermal field.

Table 2: Typical design of Paka geothermal wells

Stage of well	Depth (m)	Hole size (inch)	Casing size (inch)
Stage 1: Surface hole	0-100	26	20
Stage 2: Intermediate hole	100-350	17-1/2	13-3/8
Stage 3: Production hole	350-1200	12-1/4	9-5/8
Stage 4: Open hole	1200-3000	8-1/2	7 (Liner)

Figure 9 compares the time taken to drill wells within the Paka geothermal field. The plot shows how drilling of recent wells, especially well PW-03B, has progressed more rapidly than earlier wells. Drilling could however not proceed beyond 2791 m because high torque and drag forces that exceed the drill-pipe design limits were experienced. Overcoming this challenge is one of the motivating factors for carrying out this research.

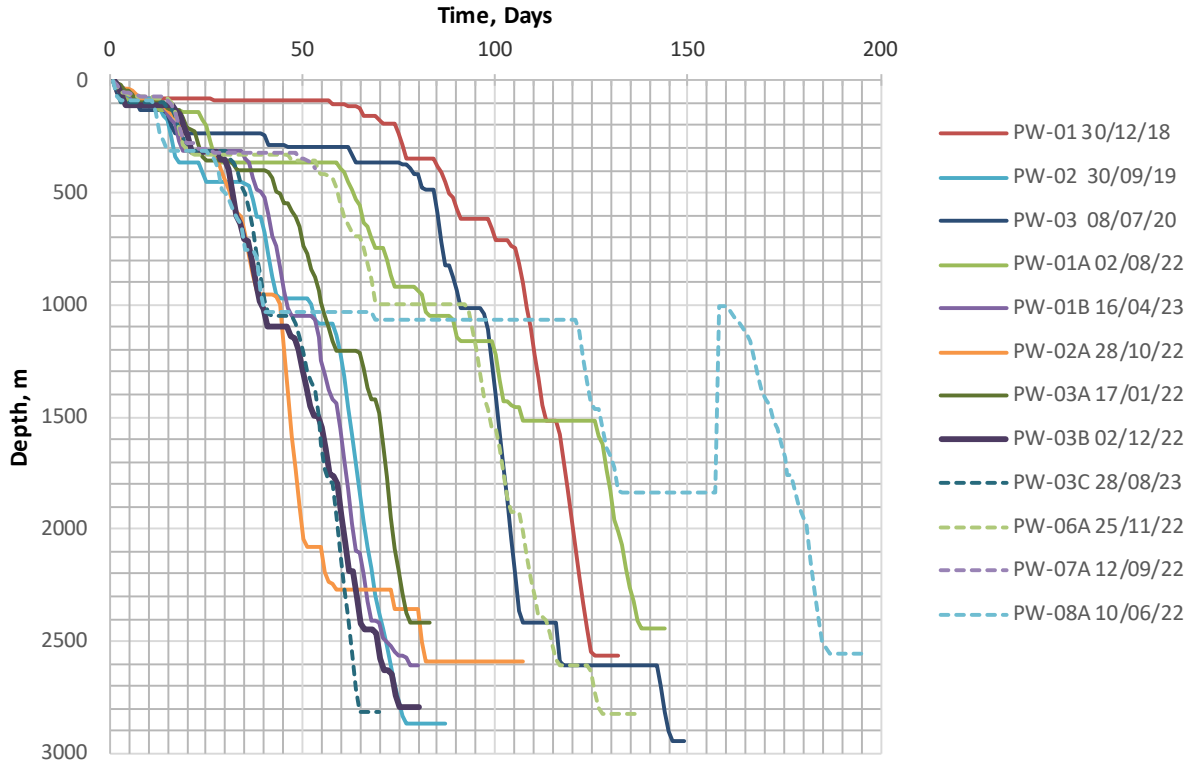

Figure 8: Drilling progress over time for wells in the Paka field, date of each well completion shown (GDC, 2022).

2.5 Research Gap and Findings from Literature Review

From the Literature review, detailed studies on the actual drilling parameters have not been done for aerated drilling. This research focuses on this area of research by using actual field data to model present drilling practices in Kenya. The aim of this research is to come up with optimum drilling parameters for aerated drilling that optimizes rate of penetration to reduce drilling time. The current average drilling time is about 100 days for a well of about 2700 m. The aim is to come up with parameters that will make it possible to reach the average drilling time of about 60 days to drill a well to a depth of 3000 m. From the study of Ong'au et al. (2010), the average drilling time for Kenyan (Olkaria field) and for Icelandic geothermal wells were about 60 and 41 days respectively for depths of 2830 m and 2379 m respectively. Data collected from well PW-03B were used in the simulation and as the basis of finding optimized parameters for Paka geothermal field.

Chapter 3

Methodology

3.1 Overview of Methods

This dissertation describes researches on the optimum well cleaning parameters while drilling a geothermal well using aerated water as the drilling fluid. The aim is to efficiently evacuate drill cuttings as they are generated by the drill bit and to transport them to the surface through the annulus. The factors that affect cuttings transportation were investigated and the best parameters singled out to be used for actual drilling scenarios.

The methodology employed to achieve the goals of the study was to simulate cuttings transportation in a manner consistent with actual drilling data collected from a well in Paka geothermal field in Baringo County, Kenya. The Transient-Cuttings-Transport (TCT) simulator was then used to recreate new drilling scenarios. The collected field data was used in calibrating the numerical simulation model. The well design data in Figure 11 was used in the simulation of cuttings transportation for well PW-03B. This research covers cuttings transport modelling for the 12-1/4″ production hole section from 308 m to 1099 m. The resultant calibrated model was used to come up with optimum parameters for drilling.

3.2 Theory of the Numerical Simulation of Cuttings Transportation

3.2.1 Numerical Simulation of Cuttings Transportation: TCT Simulator

The flow of cuttings from the bottom of the hole to the surface through the annulus is controlled by a number of forces such as gravity, buoyancy, drag, inertia, friction and inter-particle contact. The complexity of transportation of the cuttings varies depending on the well profile. Cuttings transportation in highly inclined wells and horizontal wells is more complex than in less inclined and vertical wells. In inclined wells, usually a cuttings bed forms and this makes

cuttings transportation more difficult. The following factors affect cuttings transportation through the annulus (Azar and Samuel, 2007):

- cuttings slip velocity
- cuttings properties including size, shape, density, concentration and others.
- annular fluid velocity
- flow regime of the fluid and cuttings slippage
- annular velocity profile which is dictated by the fluid rheology, eccentricity of the drill pipe and ratio of hole to drill pipe diameter
- cuttings bed formation which is common in inclined wells
- rotation speed of the drill pipe
- rate of penetration
- fluid rheological properties
- hole inclination

Movement of cuttings from the bottom of the well to the surface in an inclined well follows a complex process. Numerical simulation helps to understand and quantify the annular factors that contribute to this process. Several mathematical models have been developed over time and used to determine the required hole cleaning parameters. The model chosen for a particular well depends on the type of drilling fluid used. The following empirical correlations and models can be used:

- Empirical correlations
- Two-layer models
- Three-layer models
- Three-segment models.

The model utilized in this research is a three-phase gas-liquid-solid two-layer model as shown in Figure 9.

The Transient-Cuttings-Transport (TCT) simulator was utilized in the modelling. TCT simulates cuttings behaviour in directional wells as well as in extended reach wells that have complex trajectories. TCT implements mass and momentum conservation equations to describe multiphase flow of water/mud and solid rock cuttings particles within the annulus of a wellbore as shown in Figure 9. It can also be used to describe additional flow of air within the well (Naganawa et al., 2017).

Layer 1 consists of solid (cuttings) and liquid mixture phase. Layer 2 consists of liquid and gas phases with suspended solid particles.

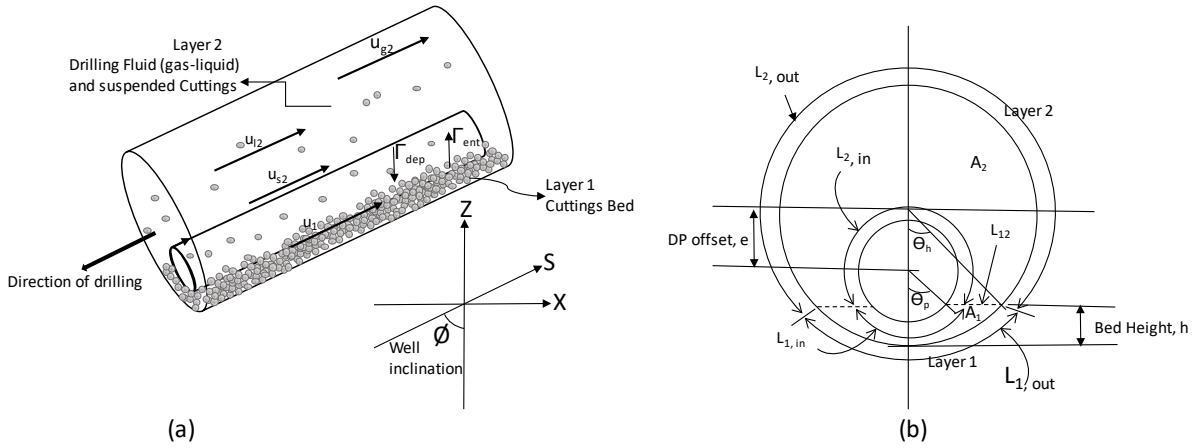

Figure 9: (a) Schematic diagram of a 3-phase, two-layer model and (b) the cross-sectional view of the variables.

From Figure 9 (a), the *S*-axis is in line with the direction of the well bore that is inclined at an angle ϕ. The horizontal displacement is in the direction of *X* and the vertical depth is in the direction of *Z*. Isothermal conditions were assumed in the derivation of the governing equations, thus, only the mass and momentum conservation were considered. In addition, basic equations of the model were derived from the geometric characteristics and also flow characteristics.

3.2.2 Governing Equations for the Three-Phase, Two-Layer Model

The original modelling considering a three-phase two-layer model was developed by Doan and Oguzutoreli (2001) which fits with aerated water drilling case used in Kenya. Naganawa et al. (2006, 2017) have done modelling to match the field drilling operating conditions as close as possible using two-phase two-layer model. This research utilizes both aspects of the models to fit the Kenyan geothermal drilling conditions in Paka geothermal field. The three-phase, two-layer model consists of two layers. Layer 1 is mixture of cuttings (solids) that form a bed and liquid that moves through it. There is continuous deposition and entrainment of cuttings to and from layer1. Layer 2 consist of solid particles, liquid and air phases and is constantly moving over layer 1.

(1) Basic Equations

The following equations provides the relationship between various variables used in the model as seen in Figure 9. Layer 1 is the cuttings bed and it forms a sedimentary layer that is assumed to be uniformly packed in a simple cubic arrangement. The assumption used in the model is that the cuttings are spherical although in real life, this is rarely the case. Cubic packing of the solids yields the following relationship:

$$C_{s1} + C_{l1} = 1 \; and \; C_{s1} = 0.52 \tag{1}$$

For Layer 2, it consists of the three phases; for the fluid phase,

$$C_{f2} = C_{l2} + C_{g2} \tag{2}$$

Considering the 3 phases in layer 2,

$$C_{s2} + C_{l2} + C_{g2} = 1 \tag{3}$$

The liquid and solid phases are incompressible while the gas phase is compressible as a function of pressure, hence:

$$\rho_s = Constant, \; \rho_l = Constant \; and \;\; \rho_g = \rho_g(p) \tag{4}$$

The mixture density of the fluid phase will be given as:

$$\rho_f = \frac{C_{l2}\rho_l + C_{g2}\rho_{lg}}{C_{f2}} \tag{5}$$

The mixture density of the solid and liquid phase in layer 1 is given as:

$$\rho_1 = C_{s1}\rho_s + C_{l1}\rho_l \tag{6}$$

The mixture density of the solid and liquid phase in layer 2 is given as:

$$\rho_2 = C_{s2}\rho_s + C_{f2}\rho_{lf} = C_{s2}\rho_s + C_{l2}\rho_l + C_{g2}\rho_g \tag{7}$$

(2) Conservation of Mass Equations

The law of conservation of mass is used to describe the movements of the various phases in both layer 1 and layer 2.

The mass conservation equation for layer 1 (mixed solid-liquid) is given as:

$$\frac{\partial}{\partial t}A_1 + \frac{\partial}{\partial s}(A_1 u_1) = \frac{1}{\rho_1}\left(\left(\Gamma_{dep,s} + \Gamma_{dep,l}\right) - \left(\Gamma_{ent,s} + \Gamma_{ent,l}\right)\right) \tag{8}$$

The mass conservation equation for layer 2 gas phase is given as:

$$\frac{\partial}{\partial t}\left(C_{g2}A_2\rho_g\right) + \frac{\partial}{\partial s}\left(C_{g2}A_2\rho_g u_{g2}\right) = \rho_g \frac{Q_{g,in}}{\Delta s} \tag{9}$$

The mass conservation equation for layer 2 liquid phase is given as:

$$\frac{\partial}{\partial t}(C_{l2}A_2) + \frac{\partial}{\partial s}(C_{l2}A_2 u_{l2}) = \frac{1}{\rho_l}\left(\Gamma_{ent,l} - \Gamma_{dep,l}\right) \tag{10}$$

The mass conservation equation for layer 2 solid phase is given as:

$$\frac{\partial}{\partial t}(C_{s2}A_2) + \frac{\partial}{\partial s}(C_{s2}A_2u_{s2}) = \frac{1}{\rho_s}\left(\Gamma_{ent,s} - \Gamma_{dep,s}\right) \tag{11}$$

The terms $\Gamma_{dep,s}$, $\Gamma_{dep,l}$, $\Gamma_{ent,s}$, and $\Gamma_{ent,l}$ are mass transfer rates between the two layers defined as:

$$\Gamma_{dep,s} = C_{s1}\rho_s L_{12}\left(\frac{C_{s2}}{C_{s1}}\right)v_{dep},\ \Gamma_{dep,l} = C_{l1}\rho_l L_{12}\left(\frac{C_{s2}}{C_{s1}}\right)v_{dep},\ \Gamma_{ent,s} = C_{s1}\rho_s L_{12}v_{ent},$$

$$\Gamma_{ent,l} = C_{l1}\rho_l L_{12}v_{ent} \tag{12}$$

(3) Conservation of Momentum Equations

The momentum conservation equation for layer 1 (mixed solid-liquid) is given as:

$$\frac{\partial}{\partial t}(A_1\rho_1u_1) + \frac{\partial}{\partial s}(A_1\rho_1u_1u_1) = -A_1\left(\frac{\partial p}{\partial s} + \rho_1 g\cos\phi\right) - \tau_1L_1 + \tau_{12}L_{12} - F_1 +$$

$$(C_{s1}\rho_s L_{12}u_{s2} + C_{l1}\rho_l L_{12}u_{12})\frac{C_{s2}}{C_{s1}}v_{dep} - \rho_1 L_{12}u_1v_{ent} \tag{13}$$

The momentum conservation equation for layer 2 (solid-liquid-gas phase) is given as:

$$\frac{\partial}{\partial t}\left(C_{s2}A_2\rho_s u_{s2} + C_{l2}A_2\rho_l u_{l2} + C_{g2}A_2\rho_g u_{g2}\right) + \frac{\partial}{\partial s}\left(C_{s2}A_2\rho_s u_{s2}u_{s2} + C_{l2}A_2\rho_l u_{l2}u_{l2} +\right.$$

$$\left.C_{g2}A_2\rho_g u_{g2}u_{g2}\right) = -A_2\left(\frac{\partial p}{\partial s} + \rho_2 g\cos\phi\right) - (\tau_2L_2 + \tau_{12}L_{12}) - (C_{s1}\rho_s L_{12}u_{s2} +$$

$$C_{l1}\rho_l L_{12}u_{12})\frac{C_{s2}}{C_{s1}}v_{dep} + \rho_1 L_{12}u_1v_{ent} \tag{14}$$

The momentum conservation equation for layer 2 (solid phase) is given as:

$$\frac{\partial}{\partial t}(C_{s2}A_2\rho_s u_{s2}) + \frac{\partial}{\partial s}(C_{s2}A_2\rho_s u_{s2}u_{s2}) = -C_{s2}A_2\left(\frac{\partial p}{\partial s} + \rho_s g\cos\phi\right) - C_{s2}(\tau_2L_2 +$$

$$\tau_{12}L_{12}) + F_{sf} - C_{s1}\rho_s L_{12}\left(u_{s2}\frac{C_{s2}}{C_{s1}}v_{dep} - u_1v_{ent}\right) \tag{15}$$

The flow of the gas phase in layer 2 and mixed (gas-liquid) flow velocity of layer 2 are given as (Uematsu, 2003)

$$u_{g2} = 0.667u_{l2}(1 + \cos\phi) \tag{16}$$

$$u_{f2} = \frac{\rho_g C_{g2}u_{g2} + \rho_l(1 - C_{s2} - C_{g2})u_{l2}}{\rho_f(1 - C_{s2})} \tag{17}$$

The final model consists of 8 simultaneous equations with 8 independent variables. The independent variables are u_1, u_{s2}, u_{l2}, u_{g2}, p, C_{s2}, C_{g2}, and A_2. To mathematically solve these equations, constitutive equations have to be introduced. Also the cutting's deposition and entrainment relationships between the layers has to be modelled.

(4) Constitutive Equations

The shear stresses experienced between the cuttings and the pipe walls at layer 1 and 2 are given as:

$$\tau_1 = \frac{1}{2} f_1 \rho_1 |u_1| u_1 \tag{18}$$

$$\tau_2 = \frac{1}{2} f_2 \rho_2 |u_2| u_2 \tag{19}$$

The friction factors are given as:

$$f_1 = \begin{cases} \frac{16}{Re_1} & Re_1 < 2{,}100 \\ 0.046 {Re_1}^{-0.2} & Re_1 \geq 2{,}100 \end{cases} \tag{20}$$

$$f_2 = \begin{cases} \frac{16}{Re_2} & Re_2 < 2{,}100 \\ 0.046 {Re_2}^{-0.2} & Re_2 \geq 2{,}100 \end{cases} \tag{21}$$

The Reynolds number for each layer is calculated as:

$$Re_1 = \frac{\rho_1 |u_1|^{2-n} {D_1}^n}{8^{n-1} \mu_1} \tag{22}$$

$$Re_2 = \frac{\rho_2 |u_2|^{2-n} {D_2}^n}{8^{n-1} \mu_2} \tag{23}$$

The drilling fluid used in drilling was aerated water hence falls under the rheological model of Bingham plastic fluid (Guo and Liu, 2011; Ozbayoglu et al., 2000) given as.

$$\tau = \tau_y + \mu_p \gamma \tag{24}$$

The Reynolds number given by the mixing rule as:

$$Re_2 = C_{g2} \frac{\rho_2 |u_{g2}| D_2}{\mu_g} + C_{l2} \frac{\rho_1 |u_{l2}|^{2-n} {D_2}^n}{8^{n-1} K} \tag{25}$$

where D_2 is the equivalent hydraulic diameter of layer 2 given as:

$$D_2 = \frac{4A_2}{L_2 + L_{12}} \tag{26}$$

The friction f_2, for the two-phase gas-liquid layer 2, is expressed as a single fluid friction f_2' multiplied by a correction factor e^s (where e is the Euler's number and s is the friction coefficient ratio) thus:

$$f_2 = e^s f_2' \tag{27}$$

Beggs and Brill (1973) in their study of gas-liquid flow in inclined circular pipes where f_{tp} is two phase friction factor and f_{ns} is the non-slip friction factor showed that:

$$\frac{f_{tp}}{f_{ns}} = e^s \tag{28}$$

where

$$s = \frac{\ln(y)}{-0.0523+3.182\ln(y)-0.8725\ln(y)^2+0.01853\ln(y)^4} \tag{29}$$

$$y = \frac{\lambda_{ns}}{\lambda^2} \text{ and } \lambda_{ns} = \frac{q_l}{q_l+q_g} = \frac{C_{l2}u_{l2}}{C_{l2}u_{l2}+C_{g2}u_{g2}}, \lambda = \frac{C_{l2}}{C_{l2}+C_{g2}} \tag{30}$$

For intervals where $1<y<1.2$, the value of s is given as:

$$s = \ln(2.2y - 1.2) \tag{31}$$

Air from the atmosphere was used in drilling. In calculating the properties of air used, real gas properties were used. Since the properties of air are dependent on pressure and temperature, the downhole properties were determined using Hall and Yarborough (1973) method.

The equation of state for one mole of real gas is given by:

$$pV = zRT \tag{32}$$

The density of the gas defined as mass per unit volume at a given temperature and pressure is given as:

$$\rho_g = \frac{pM_w}{zRT} \tag{33}$$

where z is the compressibility factor and may be determined using the Standing and Katz chart (1942). The Dranchuk and Abou-Kassem equation of state (1975) is also used in calculating z where the values $T_{pr}\neq 1$ and $p_{pr}>1$ and for gases with specific gas gravity $0.554<\gamma_g<1.862$ (Terry et al., 2015).

$$z = 1 + c_1(T_{pr})\rho_r + c_2(T_{pr})\rho_r{}^2 - c_3(T_{pr})\rho_r{}^5 + c_4(\rho_r, T_{pr}) \tag{34}$$

where

$$\rho_r = \frac{0.27 p_{pr}}{z T_{pr}},\ p_{pr} = \frac{p_R}{p_{pc}},\ \ T_{pr} = \frac{T_R}{T_{pc}},\ \ p_{pc} = 671.1 + 14.0\gamma_g - 34.3{\gamma_g}^2, T_{pc} = 120.1 + 357.7\gamma_g - 62.9{\gamma_g}^2 \quad (35)$$

where

$$c_1(T_{pr}) = 0.3265 - 1.0700/T_{pr} - 0.5339/{T_{pr}}^3 + 0.01569/{T_{pr}}^4 - 0.05165/{T_{pr}}^5 \quad (36)$$

$$c_2(T_{pr}) = 0.5475 - 0.7361/T_{pr} - 0.1844/{T_{pr}}^2 \quad (37)$$

$$c_3(T_{pr}) = 0.1056(-0.7361/T_{pr} - 0.1844/{T_{pr}}^2) \quad (38)$$

$$c_4(\rho_r, T_{pr}) = 0.6134(1 + 0.7210{\rho_r}^2)({\rho_r}^2/{T_{pr}}^3) exp(-0.7210{\rho_r}^2) \quad (39)$$

The viscosity of the gas phase is calculated using the method developed by Lee et al. (1966),

$$\mu_g = 10^{-4} K exp(X {\rho_g}^Y) \quad (40)$$

$$K = \frac{(9.379 + 0.01607 M_w) T^{1.5}}{209.2 + 19.26 M_w + T} \quad (41)$$

$$X = 3.448 + \frac{986.4}{T} + 0.01009 M_w \quad (42)$$

$$Y = 2.447 - 0.2224X \quad (43)$$

The multi particle drag force between the cuttings and the fluid layer is calculated using Shook and Roco (1991) method.

$$F_{sf} = C_{s2} A_2 \frac{3 C_D \rho_l |u_{l2} - u_{s2}| (u_{l2} - u_{s2})}{4 d_p (1 - C_{s2})^{1.65}} \quad (44)$$

where the drag coefficient C_D is given as

$$C_D = \begin{cases} \frac{24}{Re_p}\left(1 + 0.15 {Re_p}^{0.687}\right) & Re_p < 1000 \\ 0.44 & Re_p \geq 1000 \end{cases} \quad (45)$$

and the particle Reynolds number is given as

$$Re_p = C_{g2} \frac{\rho_g |u_{g2} - u_{s2}| d_p}{\mu_g} + C_{l2} \frac{\rho_{gl} |u_{l2} - u_{s2}|^{2-n} {d_2}^n}{8^{n-1} K} \quad (46)$$

The terminal velocity v_p for a single spherical drill cutting is given as:

$$v_p = \left\{\frac{4 d_p g (\rho_s - \rho_l) \sin\varphi}{3 \rho_l C_D}\right\}^{0.5} \quad (47)$$

The drag coefficient is given in equation 45 where the Reynolds number is:

$$Re_2 = C_{g2}\frac{\rho_2|v_p|d_p}{\mu_g} + C_{l2}\frac{\rho_1|v_p|^{2-n}{d_2}^n}{8^{n-1}K} \tag{48}$$

The terminal deposition velocity of the cuttings is given as

$$v_{dep} = v_p(1 - C_{s2})^m \tag{49}$$

where the variable m is calculated as:

$$m = \begin{cases} 4.45{Re_{dep}}^{0.1} & Re_{dep} < 500 \\ 2.39 & Re_{dep} \geq 500 \end{cases} \tag{50}$$

The Reynolds number Re_{dep} due to the deposition velocity v_{dep} is given as

$$Re_{dep} = C_{g2}\frac{\rho_2|v_{dep}|d_p}{\mu_g} + C_{l2}\frac{\rho_1|v_{dep}|^{2-n}{d_2}^n}{8^{n-1}K} \tag{51}$$

The entrainment rate of cuttings is given as:

$$v_{ent} = \begin{cases} m_{ent}(u_{12} - {u_{12}}^*) & u_{12} > {u_{12}}^* \\ 0 & u_{12} \leq {u_{12}}^* \end{cases} \tag{52}$$

where,

$$u_{12} = \left(\frac{\tau_{12}}{\rho_l}\right)^{0.5} = \left(\frac{f_{12}}{2}\right)^{0.5}|u_{l2} - u_1| \tag{53}$$

From equation 52, the resultant slope (m_{ent}) and the critical friction velocity (${u_{12}}^*$) were adjusted according until the simulation cuttings concentration and experimental/measured cuttings concentration match (Uematsu, 2003).

3.2.3 Rheology of the Drilling Fluid used in the Model

Drilling fluids are classified according to their flow behaviours and five models have been documented as shown in Figure 10. These models from Figure 10 are identified as the Newtonian (a), Bingham plastic (b), pseudo-plastic (c), yield power-law (also known as the Herschel-Bulkley) (d), and the dilatant (e) (Guo and Liu, 2011).

It is worth noting that Guo and Liu (2011) stated that that a foam drilling model from the work of Ozbayoglu et al. (2000) could be better characterized by using a power-law model for 0.7 and 0.8 foam qualities and a Bingham plastic model give better fit for a 0.9 foam quality. The drilling fluid used in Kenyan wells under this study is usually aerated water and foam and

the model in this research was done using the Bingham fluid model. The equation governing this model is as shown in Equation 24. The drilling fluid used was a three-phase aerated water and solids which closely matches the Bingham plastic model. The model simulated is a three-phase, two-layer model that consists of two layers. A Bingham plastic rheology is used for the liquid phase, and a two-phase friction factor between the liquid and gas phases is also considered in the model.

Table 3 shows the surface properties of the drilling fluid used in the model. As described before, the drilling fluid is dealt with as a three-phase solid, liquid and air mixture with two layers in the model.

Table 3: Densities of drilling fluid component used.

Fluid	Density	Unit
Water	1	g/cm^3
Air	1.3×10^{-3}	g/cm^3

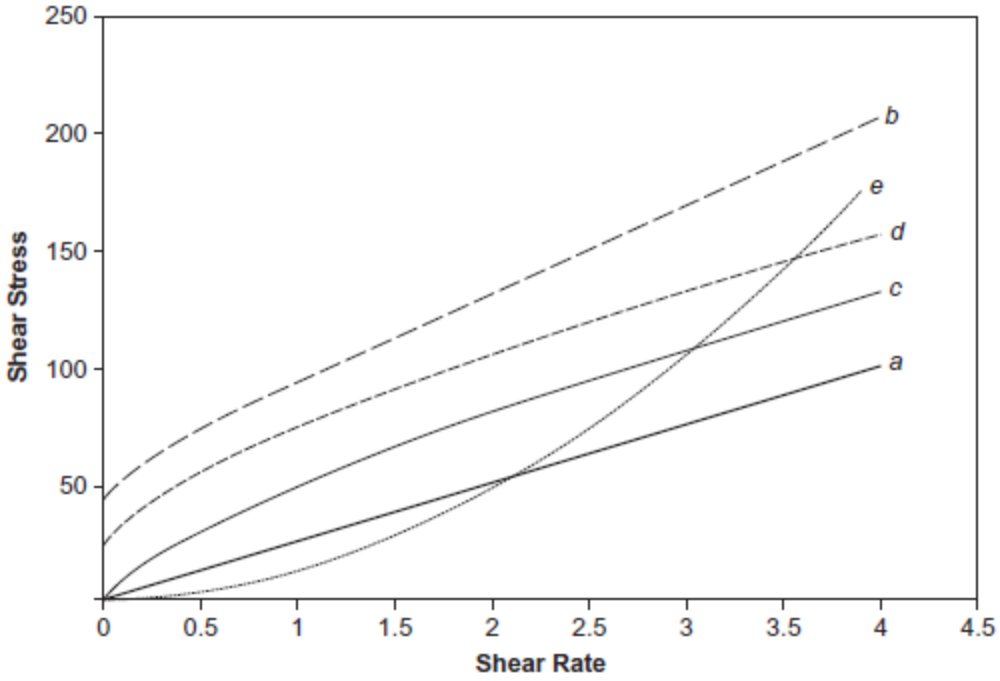

Figure 10: Rheological models (Guo and Liu, 2011).

3.3 Data from Well PW-03 Paka Geothermal Field

3.3.1 Stratigraphy of Well PW-03B

Collection of cuttings for the wells in Paka field was done after every 2 m of drilling and logged by geologists. Logging indicated that the surface section of the well mainly contained pyroclastic and trachyte rocks. The intermediate hole was mainly tuff with occasional trachyte intercalations. The production hole was mostly trachyte rock occasionally with basaltic rocks.

There were several loss zones both for the surface, intermediate and production holes. Figure 11 shows the stratigraphy of the entire well. It also shows the temperature and pressure profiles taken on different dates after drilling was completed.

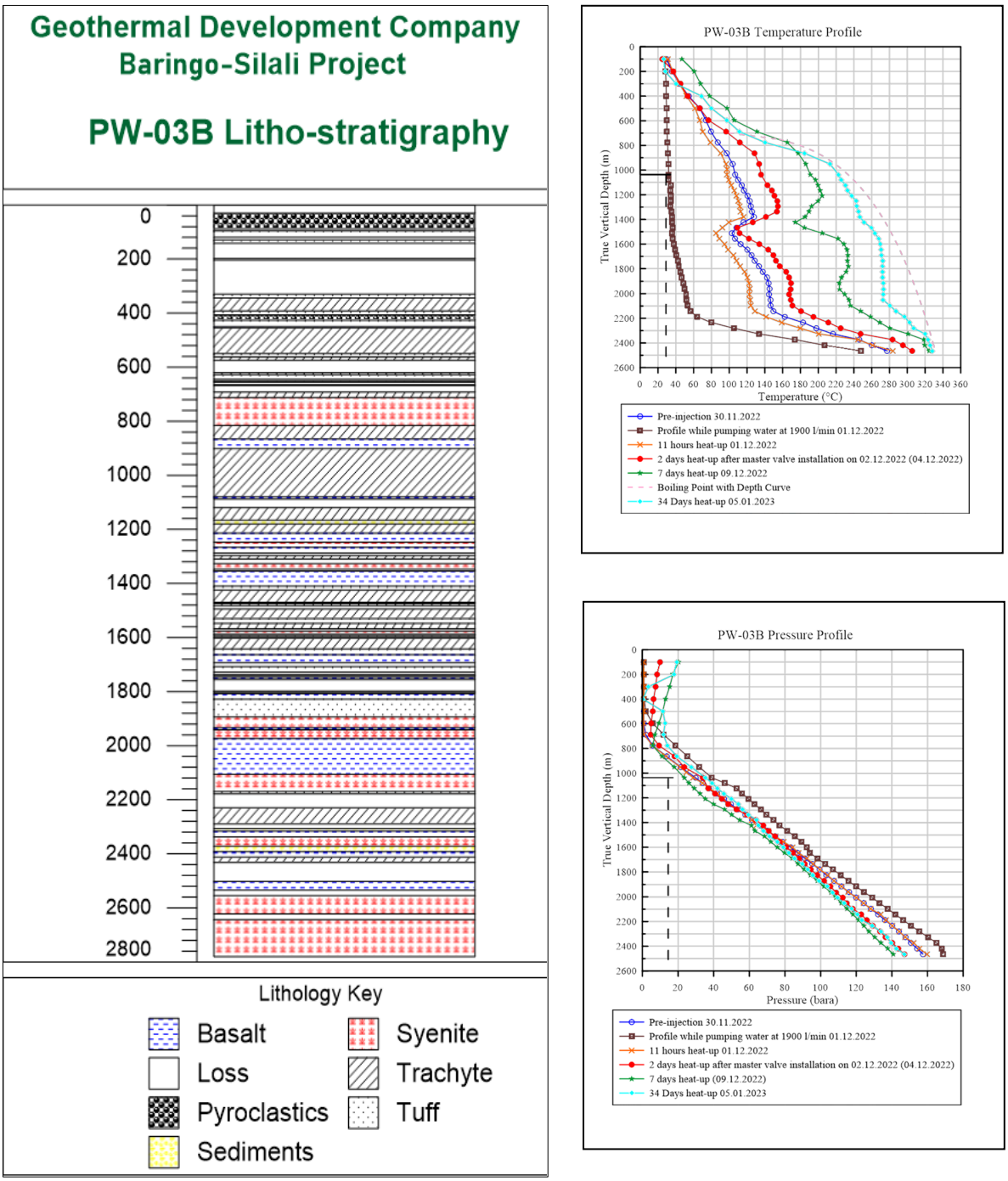

Figure 11: Litho-stratigraphy, temperature profile and pressure profile figures for well PW-3B (GDC, 2022).

3.3.2 Profile of Well PW-03B

Well PW-03B is a directional well that was drilled to a depth of 2791 m with a maximum inclination angle of about 32°. The well was spudded on the 16th of September 2022 and was completed on the 2nd of December 2022 after 78 days. High torques and drag forces were experienced towards the completion depth. The well was terminated when those two

parameters exceeded the design strength limit of the drill pipes. Figure 12 shows the well profile of PW-03B as drilled.

<table>
<tr><th>Hole Size</th><th>Drilled Depth</th><th>WELL PW-003B</th><th>Type & Size of casing</th><th>Casing shoe Depth</th></tr>
<tr><td colspan="2">Class 900, 10 Inch master valve installed</td><td rowspan="11"> 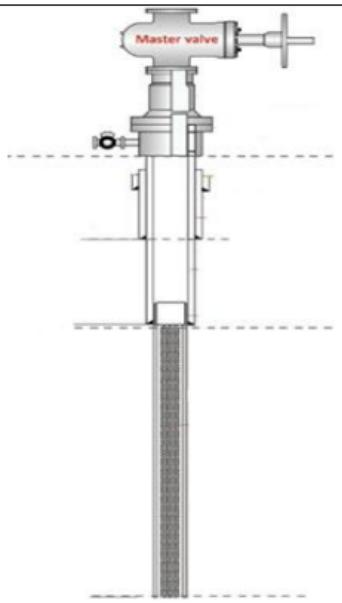
</td><td colspan="2"></td></tr>
<tr><td colspan="2"></td><td colspan="2"></td></tr>
<tr><td>26″</td><td>107m</td><td>20″ Surface</td><td>102.9m</td></tr>
<tr><td>17½″</td><td>315m</td><td>13⅜″ Anchor</td><td>308.2m</td></tr>
<tr><td colspan="2"></td><td colspan="2"></td></tr>
<tr><td colspan="2">Top of liner = 1024m</td><td colspan="2"></td></tr>
<tr><td>12¼″</td><td>1099m</td><td>9⅝″ Production</td><td>1094m</td></tr>
<tr><td colspan="2"></td><td></td><td></td></tr>
<tr><td>8½″</td><td>2791m</td><td>7″ Liners</td><td>2743m</td></tr>
</table>

Figure 12: Profile of well PW-03B (GDC, 2022).

3.3.3 Drilling Fluids for Well PW-03B

The fluids used in drilling well PW-03B were water, bentonite mud, and foam that consists of water, air and detergent. The surface section was mainly drilled with bentonite mud and occasionally with water when total fluid losses were encountered. Whenever water was used to drill, Hi-Vis mud (high viscosity sweep mud) was used for sweeping the hole before connecting a new pipe. The intermediate and production sections of the well were drilled with foam. For the Paka field, the intermediate, production and openhole sections of the well are the ones that pose a big challenge. These sections are generally associated with frequent stuck pipes, and high torque and drag forces.

The intermediate section has the advantage of having the option of using Hi-Vis bentonite mud to address some of the challenges. There is also the option of performing cement plug jobs to seal off problematic sections. In contrast, the production and open hole sections encountered frequent stuck pipes, and high torques and drag forces. Thus, the production and open hole

sections were chosen as the sections that were modelled for cuttings transportation. This study deals with the production section that has a 12-1/4″ hole diameter. The production section has a 12-1/4″ hole diameter and a casing diameter of 9-5/8″.

3.4 Data Collection

To validate the simulations, drilling data was collected from well PW-03B as drilling was ongoing in the field. Cuttings from the well were collected and measured at the shale shakers for every drill pipe joint drilled. Other data collected include the rate of penetration (ROP), revolutions per minute (RPM) of the drill string, fluid flow rate, fill of cuttings at the bottom hole, and directional drilling data.

3.4.1 Cuttings Collection and Measurement

Figure 13 shows cuttings collection and measurement at the shale shakers and the Geothermal Development Company (GDC) drilling rig.

Figure 13: Data collection at well site during drilling at Paka geothermal field. The two images on the left show the shale shakers where the drill cuttings were collected. The third image shows the weighing of collected cuttings, and the rightmost image shows the drilling rig.

3.4.2 Drilling History Data

The drilling data acquisition and monitoring system had a problem and some data had to be manually captured from the drilling history log in collaboration with the drillers. Figure 14 shows a screen shot of daily data, so called daily drilling report, captured for every single drill pipe drilled. Data captured includes the drill pipe rotation speed and advance speed, loss of circulation zones, change in formation hardness and others.

Figure 14: Drilling history data manually captured.

3.4.3 Bottom Hole Cuttings Fill

After drilling each drill pipe, the well was circulated for between 30 and 45 minutes before adding a new drill pipe to drill ahead. Each time before drilling ahead, the bottom of the hole was sounded to check if there was any fill. Fill is the cuttings unremoved by the drilling fluid circulation and remained at the bottom of the hole. Figure 15 shows the cuttings fill history. It was noted that fill was mainly encountered after stopping to conduct a deviation survey or after pulling out of the hole. In most cases, however, there was no fill.

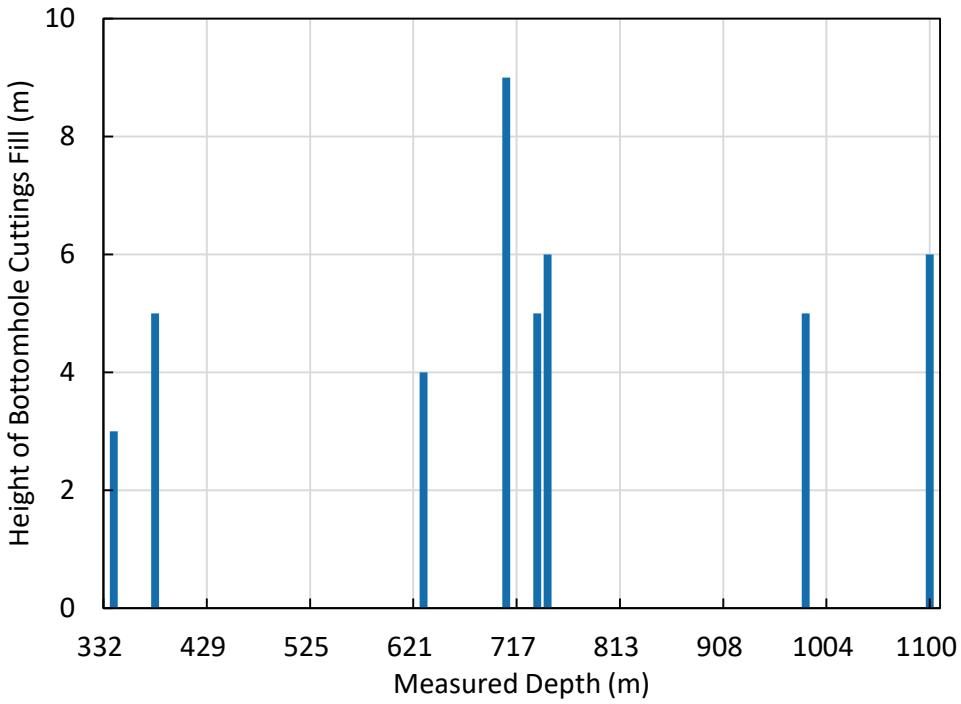

Figure 15: Fill characteristics for drilling of well PW-03B.

3.4.4 Rate of Penetration with Depth

In selecting drilling bits, formation drillability plays an important role. Mostly, formations with high drillability will require soft formation bits and those with low drillability will require hard formation bits (Ford, 2004). Paka geothermal field has high drillability formations and with optimum parameters and a proper cuttings transportation setup, high penetration rates (ROPs) can be achieved. There are also quite a lot of instances of drill pipes getting stuck mostly due to insufficient hole cleaning. Figure 16 shows the recorded ROP history along the trajectory of well PW-03B.

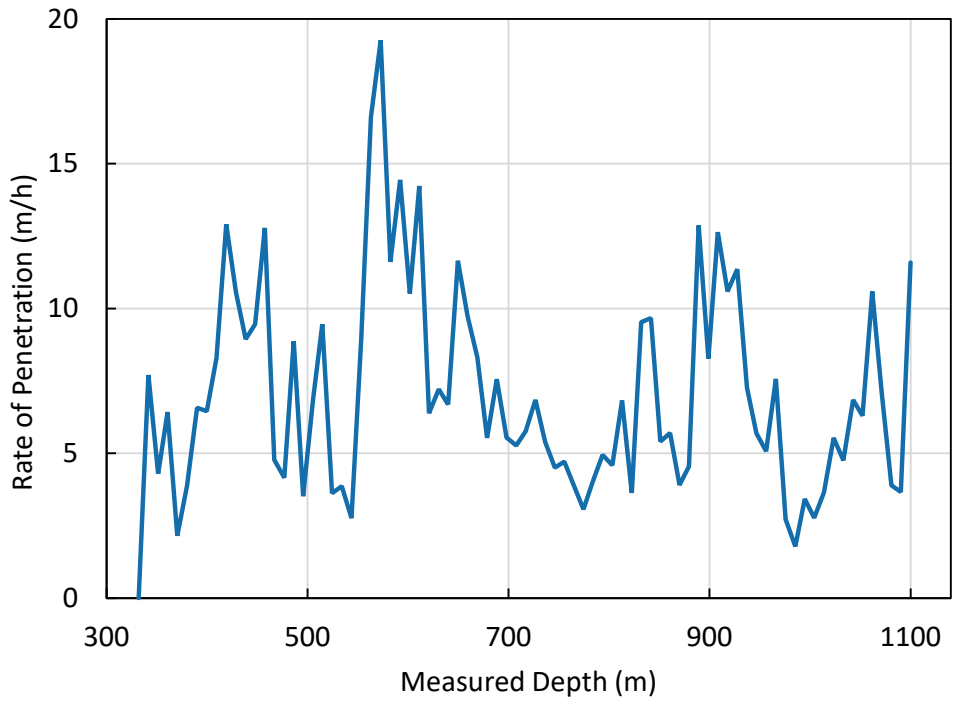

Figure 16: Rate of penetration (ROP) during drilling for well PW-03B.

3.4.5 Water Pumping Rates and Air Flow Rates

Actual pumping rates of both air and water while drilling PW-03B were as follows. In drilling the well from 332 m to 1100 m, two compressors that delivered air at 1529 Nm^3/hr (normal cubic meters per hour) at 2.4 MPa were used. The rig had three triplex mud pumps with specifications as shown in Table 4.

Table 4: Specification of mud pump used in Paka geothermal field.

Description	Quantity	Unit
Triplex Mud Pump	3	Number
Maximum Strokes Per Minute (SPM)	120	SPM
Liner Diameter	7	Inches
Stroke Length	305	mm
Maximum Pump Pressure	34.5	MPa
Pump Horsepower	1600	hp

Figure 17 shows the amount of water that was pumped at a given depth while drilling. This water containing drilling detergent was then mixed with air to form a uniform foam at the standpipe and pumped down the drill string.

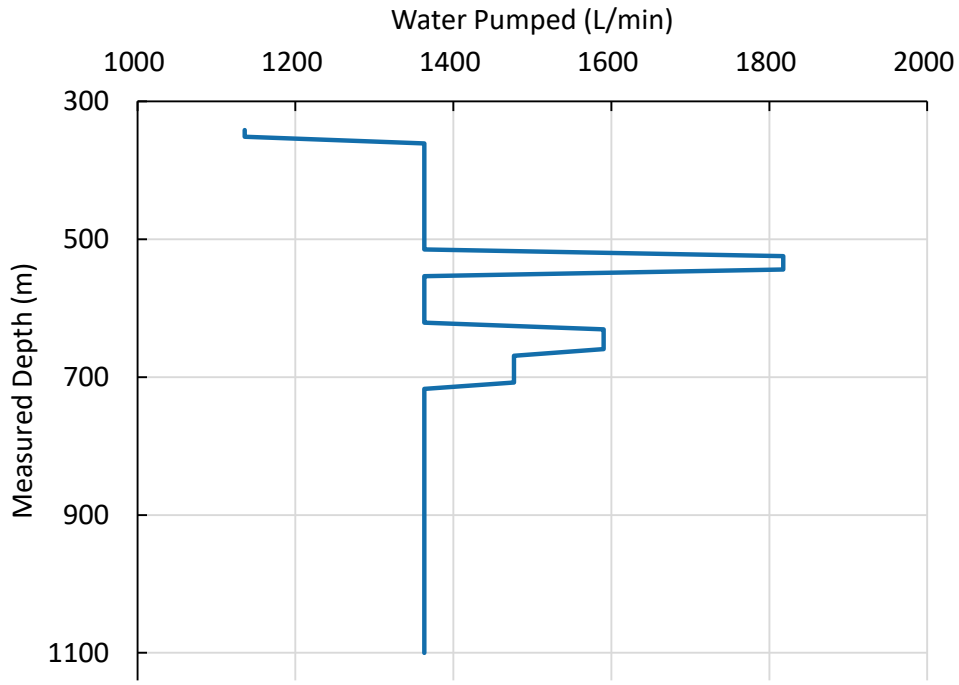

Figure 17: Water pumped while drilling PW-03B.

Chapter 4

Cuttings Transport Simulation

In a bid to understand the behaviour of cuttings movement within the wellbore annulus, several parameters were modelled. These are simulated returned cuttings, the cuttings bed height within the wellbore trajectory, cuttings concentration along the wellbore, equivalent circulating density (ECD) along the wellbore, and volumetric air rate along the wellbore.

4.1 Results of Cuttings Transport Simulation

4.1.1 General Well Profile and Cuttings Deposition in the Wellbore

It was noted that the wellbore was generally clear of cuttings as shown in Figures 18 and 19. The simulation results in Figures 18 and 19 showed that the wellbore had an insignificant amount of retained cuttings and the cuttings' bed height was small. This scenario may be attributed to long circulation times between drill pipe additions, which was factored in the simulation as periods drilling at zero ROP. A large cuttings bed height is usually a common phenomenon in highly inclined wells and extended reach wells (ERW) (Naganawa and Okatsu, 2008). Well PW-03B, on the other hand, is a moderately inclined well.

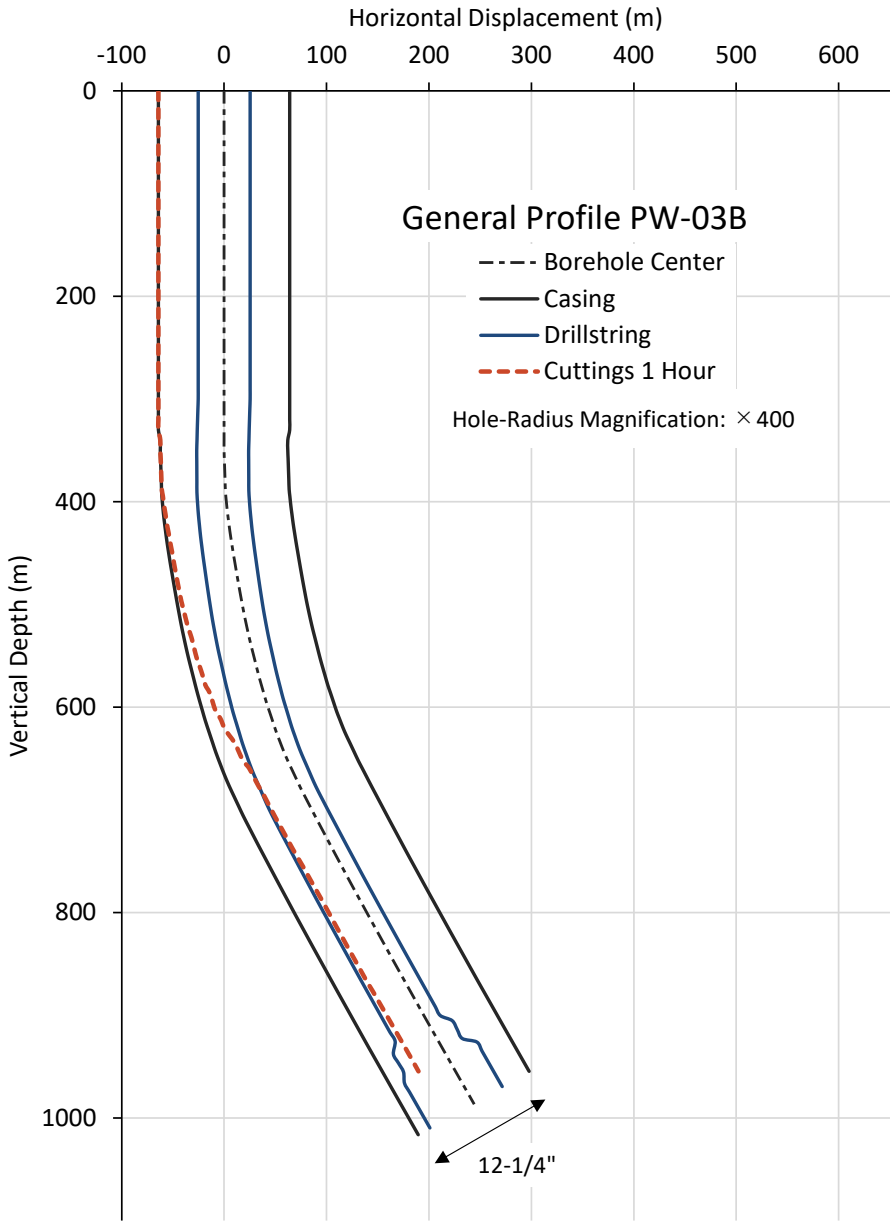

Figure 18: The well profile and the simulated cuttings deposits along the wellbore.

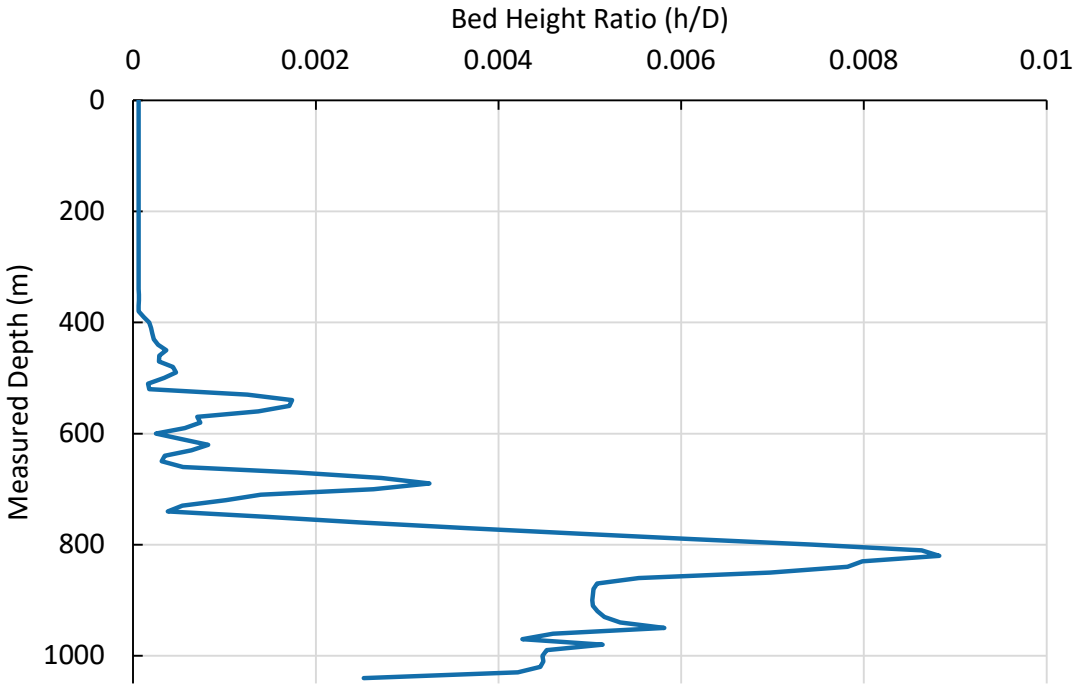

Figure 19: Simulated ratio of cuttings' bed height *h* to the hole diameter *D* along the wellbore.

4.1.2 Returned Cuttings

Cuttings from the wellbore were collected and measured in the field as drilling was going on. The model also simulated the returned cuttings. Figure 20 compares the measured cuttings returns in the field with the simulated cuttings returns and ideal cuttings returns for perfect, instantaneous cleaning. The ideal cumulative cuttings returns were calculated with the assumption that the wellbore was at gauge throughout the trajectory and that all cuttings are transported out of the hole instantaneously.

The simulated cuttings results showed more cuttings transported to the surface than the ideal case. It is expected the simulated returns to trend below the ideal scenario if influx of fluid and cuttings into the hole is not considered. To try to simulate the field scenario as close as possible, the drilling time together with circulation time were used as the input into the simulator. At times circulation time was long and this has an effect in contributing to more simulated cuttings as show in Figure 20. The TCT simulator can be used to account for hole enlargement effects; whereby the cuttings returns will be higher than the case of a perfect gauge hole (e.g., due to caving in of unconsolidated sections), and loss zones.

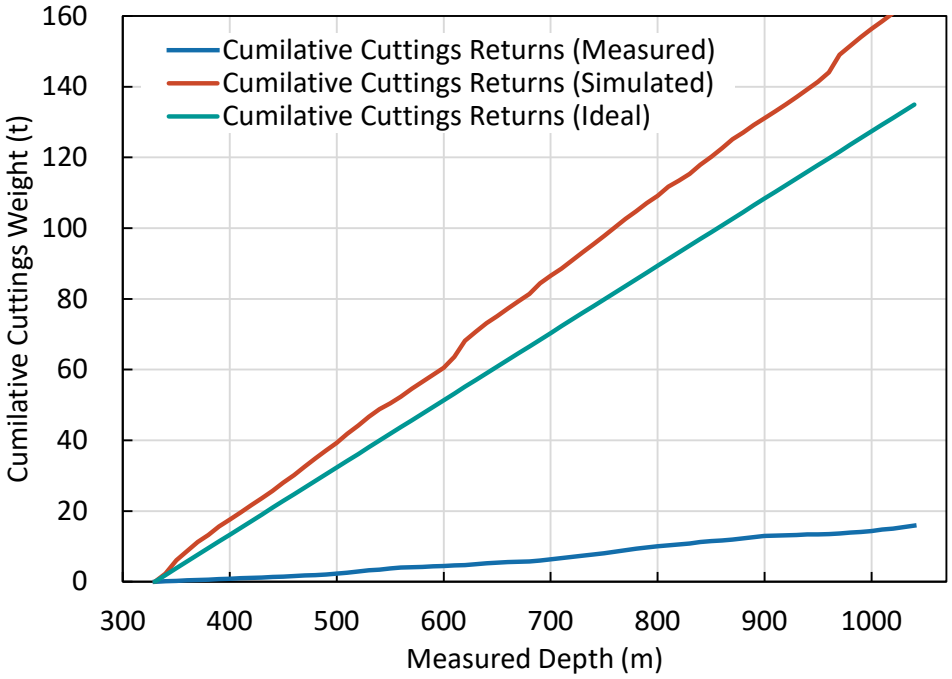

Figure 20: The cumulative cuttings characteristics.

The data from the field showed that only a small fraction of the generated cuttings was returned to the surface (Figure 20). The lower-than-expected cuttings returns to the surface can in part be explained by the fact that not all the surface cuttings were collected and measured due to surface loss on one part and also due loss into the formation during drilling. Nevertheless, the lost drill cuttings on the surface were relatively insignificant. Based on that assumption, these results indicate that a considerable amount of cuttings were lost downhole into fractured or permeable formations. This is due to numerous faults that were discussed in section 2.4.1.

4.1.3 Velocity Characteristics

It is generally accepted that a minimum annular solid velocity of about 0.25 m/s is satisfactory for cuttings transport for a typical drilling fluid (Bourgoyne et al., 1991). From the simulation, this was achieved as shown in Figure 21. The velocity of the cuttings and the fluid phases are as shown. As shown, the minimum liquid phase velocity was above 0.4 m/s.

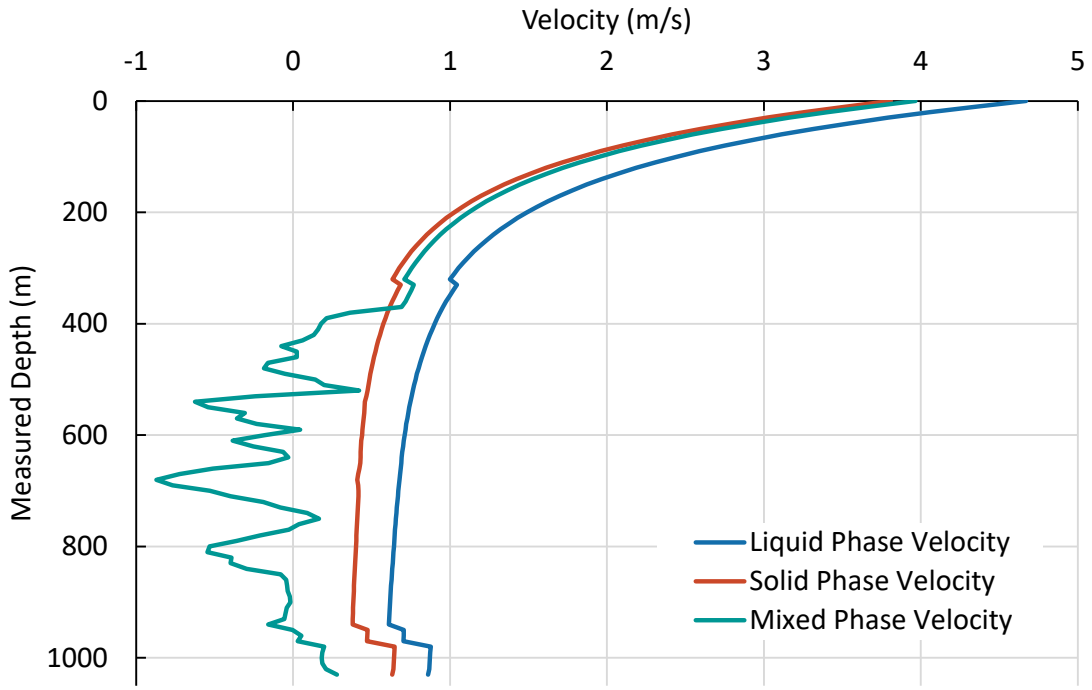

Figure 21: Velocity profiles of the fluid phases within the annulus.

4.1.4 Equivalent Circulating Density (ECD)

Depending on the depth, the column pressure of a drilling fluid may fracture the formation and induce fluid losses during drilling. A safe ECD must be maintained if loss of circulation is to be avoided. Values of ECD of about 1550 kg/m^3 may fracture some formations at quite shallow depths of less than 2000 m (Zhang and Yin, 2017). The maximum ECD for the simulation was quite low as seen in Figure 22 because of the aerated water used as the drilling fluid. This indicates that there is room for generating more cuttings at a higher rate without fracturing the formation leading to losses.

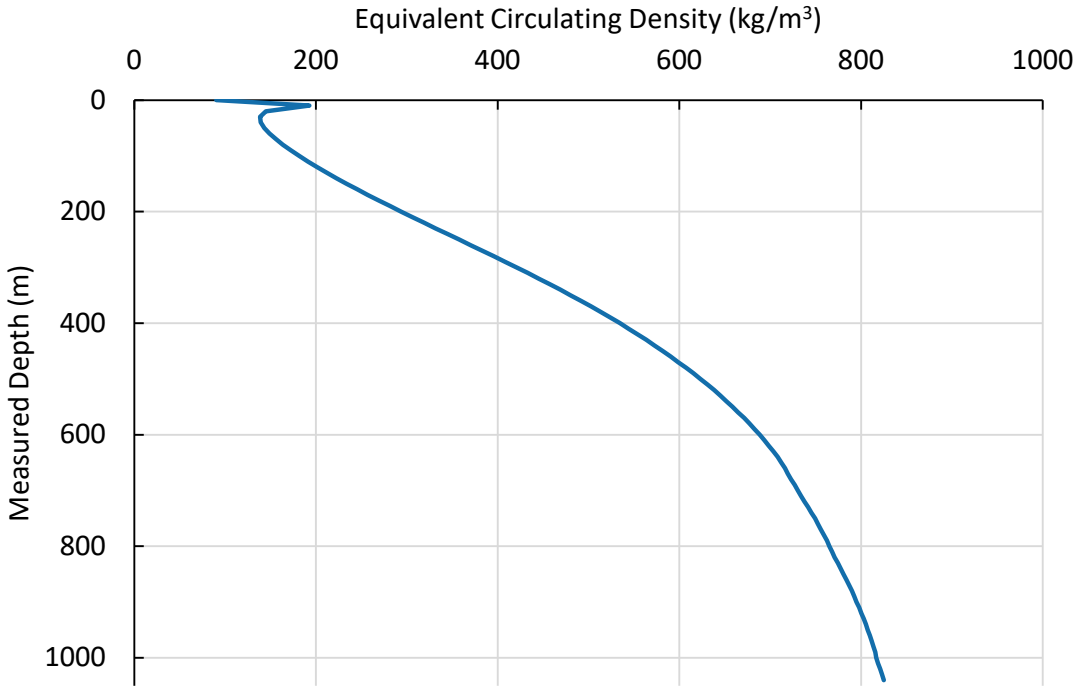

Figure 22: Variation of equivalent circulating density (ECD) with depth.

4.2 Cuttings Bed Behaviour along the Wellbore during Drilling: Drilling with Air and without Air

One indication of cuttings transportation effectiveness is the presence or absence of a cuttings bed height. Bed heights are common in horizontal and highly inclined wells. Cuttings bed heights increase pipe drag against the wellbore and also limits the sliding of the drill pipe when using mud motors in drilling. The bed height ratio is the fraction of the height of the cuttings bed (h) to the diameter of the well (D). High bed height ratios are indicative of ineffective cuttings transportation which may lead to downhole problems. Figure 23 shows the simulated bed height characteristics at chosen depths along the well bore using drilling parameters for aerated drilling. To show effectiveness of air, a simulation without air was also carried out for comparison. This simulation showed that the bed height ratio is about 10 times more when drilling with water only. This implies aerated water is much more effective in cuttings transportation than using water only.

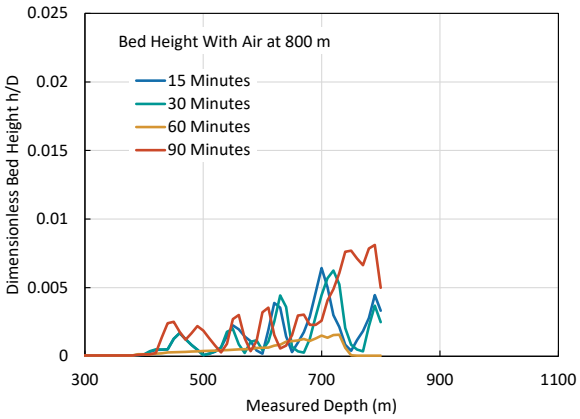

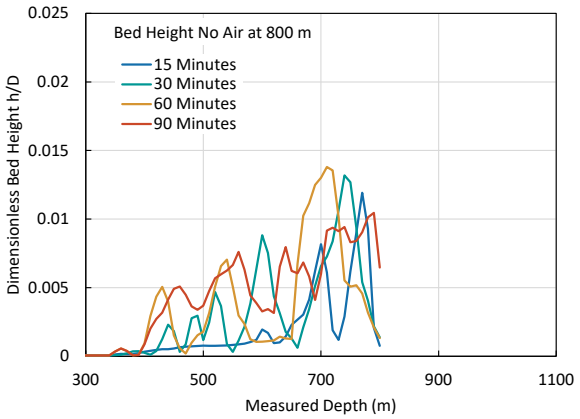

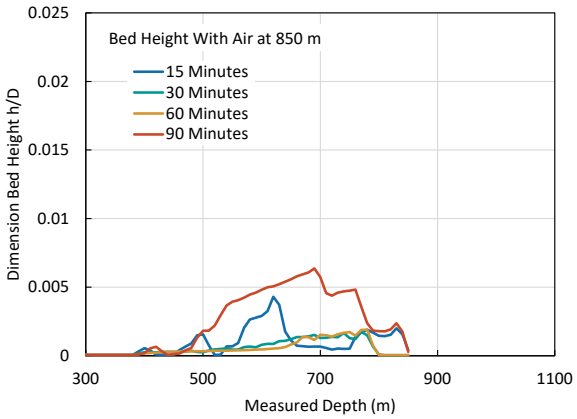

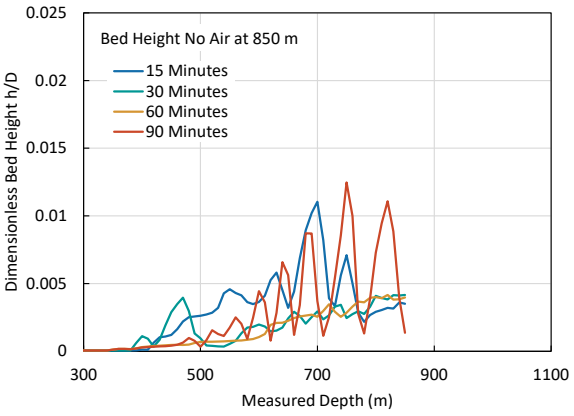

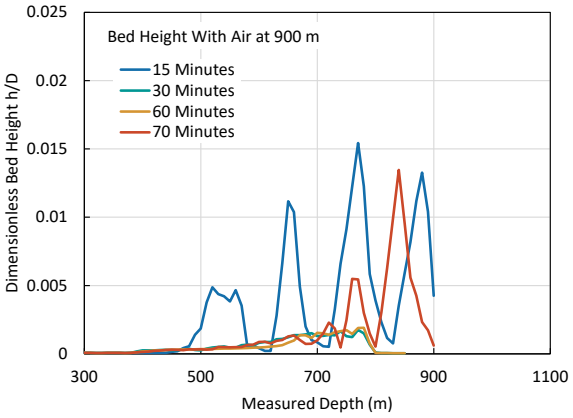

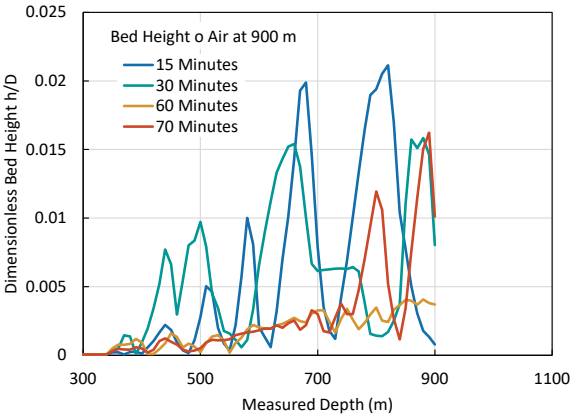

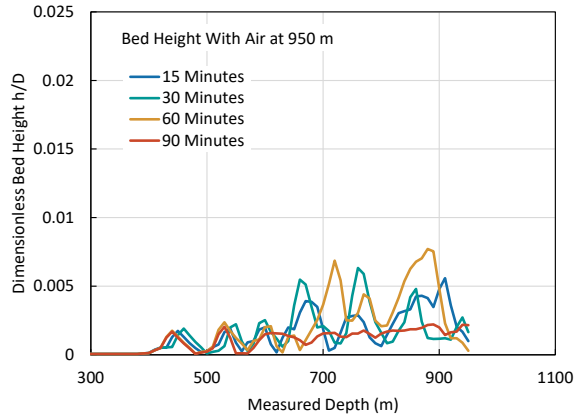

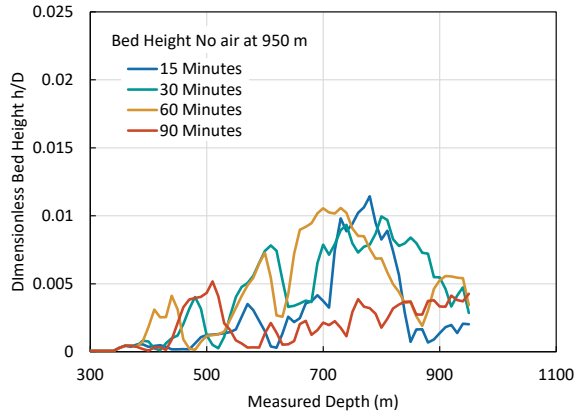

(Continued on next page)

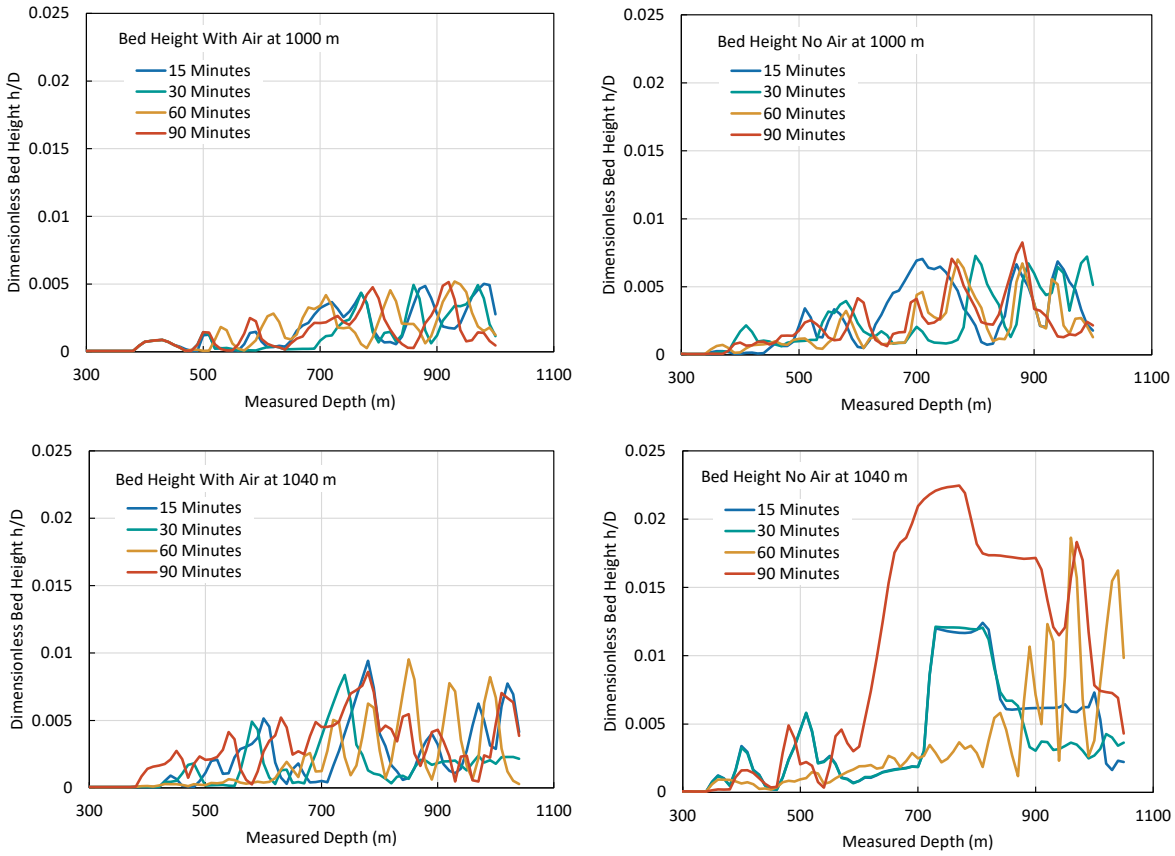

Figure 23: Variation of bed height drilling with aerated water (Left) and water only drilling (Right).

4.3 Calibrating the Model to Match Field Data

Cuttings were collected and weighed while drilling was ongoing. To compare the model and the field data, a simulation of the drilling process using the field drilling parameters was done and the comparison is as shown in Figure 20. In order to determine optimum operating parameters, the model has to be calibrated to match the field conditions. This was done by introducing loss zones by trial and error until the simulated cuttings returns matched closely with the measured cuttings returns. The final model is as shown in Figure 24 whose simulated cuttings returns matches closely with the measured cuttings returns.

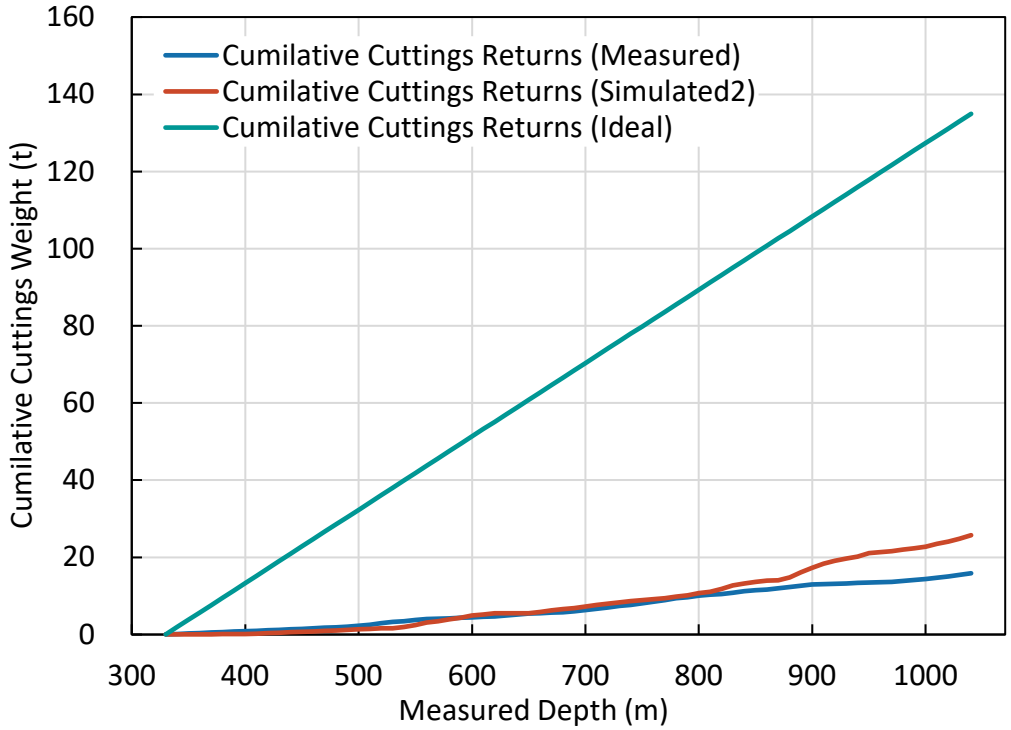

Figure 24: Calibrated model.

Chapter 5

Discussion

5.1 Optimum Pumping Rates and Air Flow Rates using the Calibrated Model

Different pumping rates were used to model the cuttings bed height within the wellbore. The results are as shown in Figures 25 to 28. At a given water pumping rate, airflow rate was varied starting with a minimum flow rate to a maximum air flow value and the bed height behaviour was observed. The depth considered for the simulation was the depth just above the bottomhole assembly (BHA) where the drill pipe starts, from 985 m to1008 m. The rate of penetration (ROP) and pipe rotation speed (RPM) were kept constant at 15 m/hr and 50 rev/min respectively and a simulated drilling time of 90 minutes.

The cuttings bed height ratio (h/D) was used to monitor the effectiveness of the various parameters used in the model. Erge and van Oort (2020), in their research of cuttings bed height that is safe during drilling and also while pulling out of hole, showed that it mostly was in the range of 0.01 and 0.015. Higher ratios may be encountered which will necessitate more circulation of the drilling fluid to ensure reduction of the bed height.

From Figures 25 to 28, the parameters that are chosen for effective cuttings transportation are those whose bed height ratio is below 0.015. The ratio is chosen as per Erge and van Oort (2020) work and also because when the simulation of the drilling process was done as close as possible to the field data, the bed height ratio was below 0.015 as seen in Figures 23. This proved safe when drilling in this section. Therefore, flow rates of 1800 l/min and air flow rates of 700 scfm and above are recommended for optimal drilling.

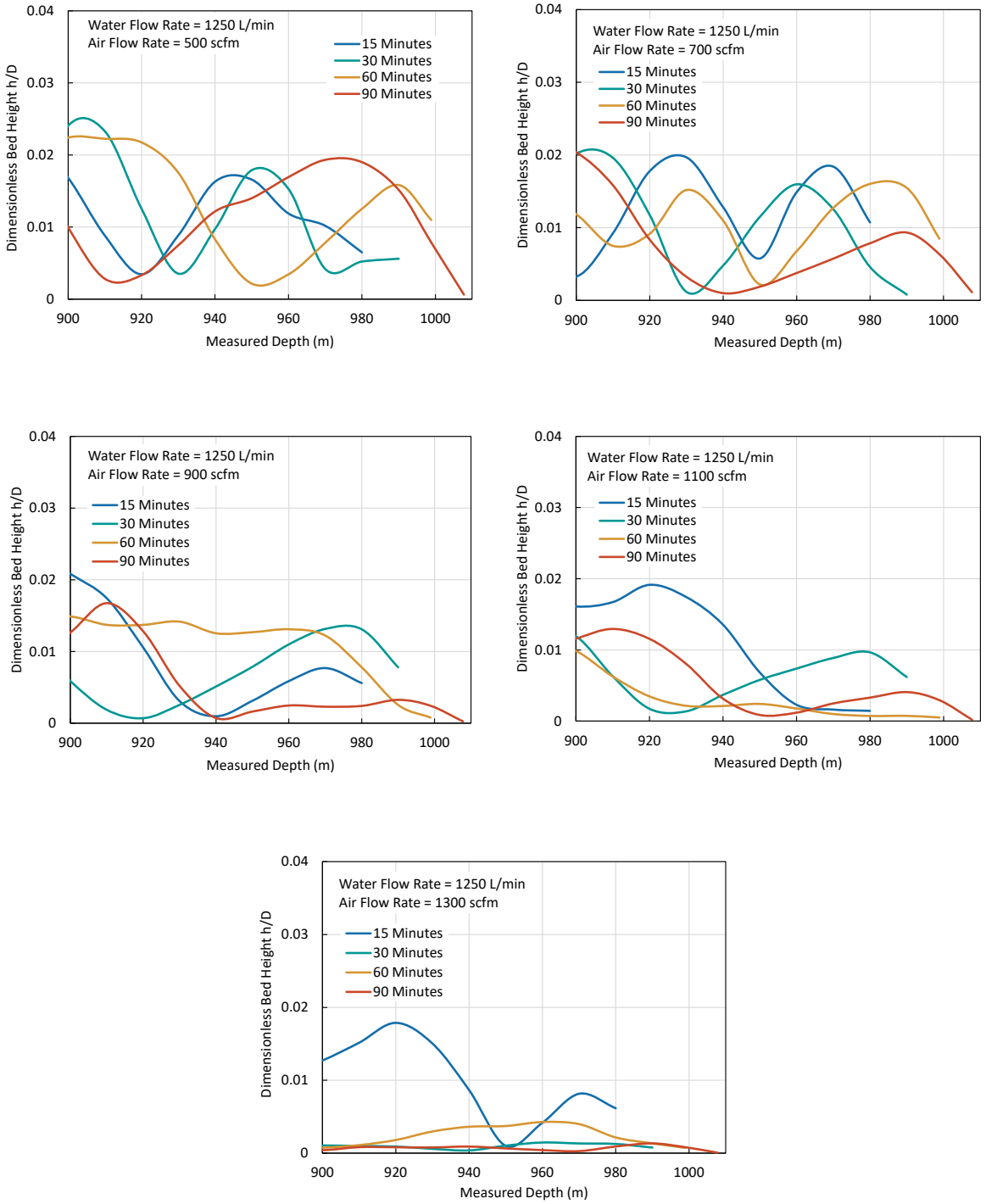

Figure 25: Bed height characteristics for 1250 l/min water with air flow rates 500-1300 scfm.

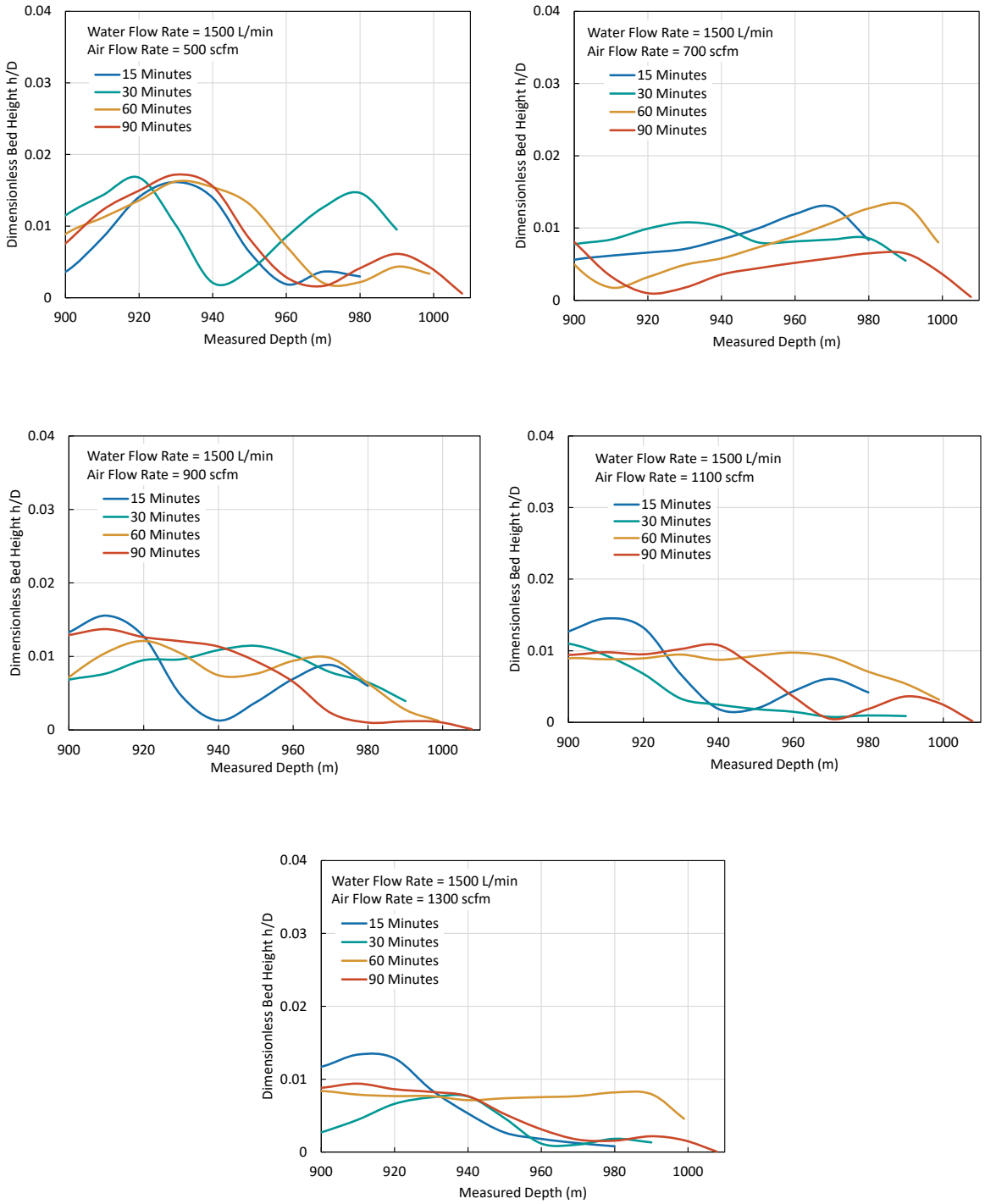

Figure 26: Bed height characteristics for 1500 l/min water with air flow rates 500-1300 scfm.

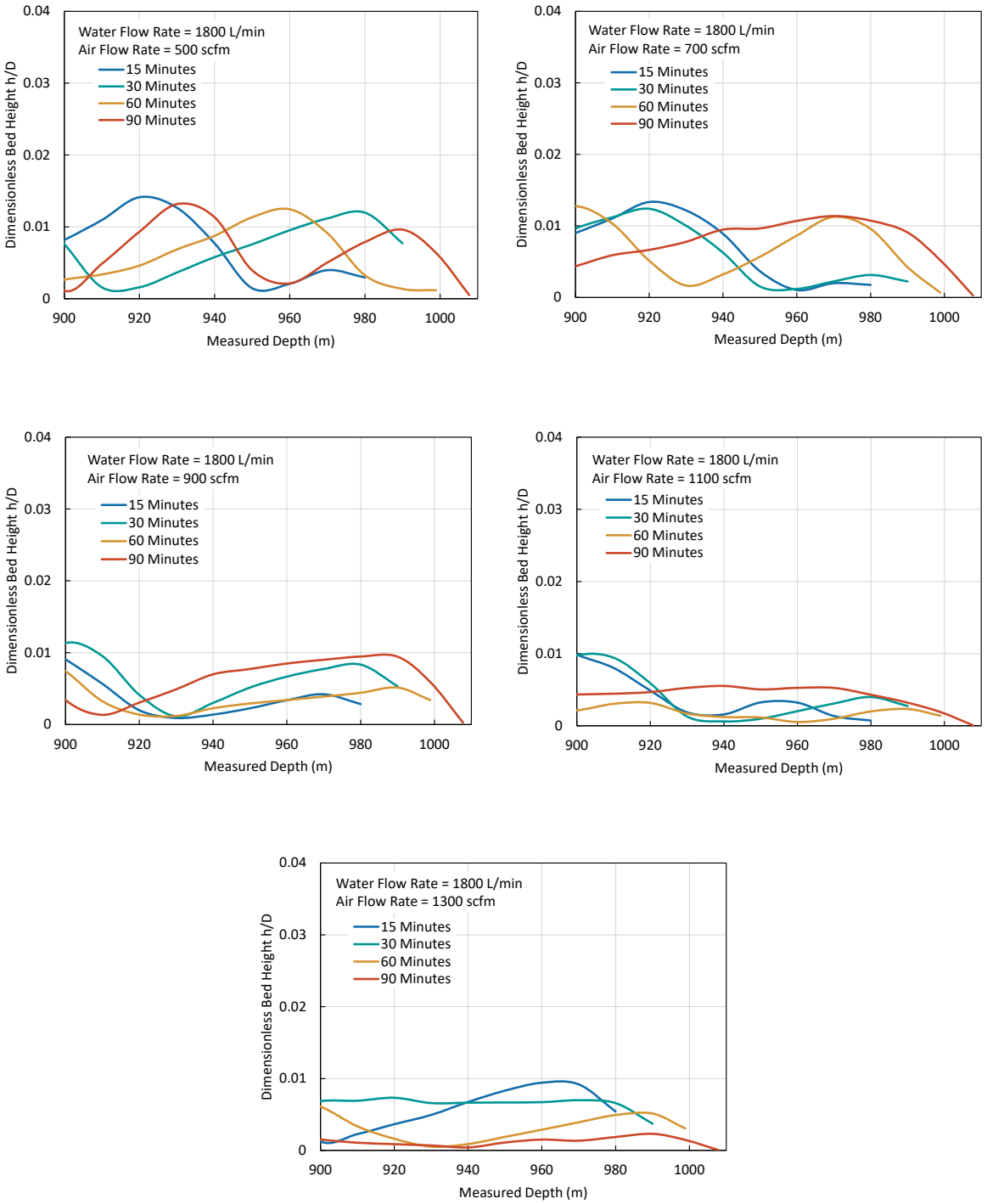

Figure 27: Bed height characteristics for 1800 l/min water with air flow rates 500-1300 scfm.

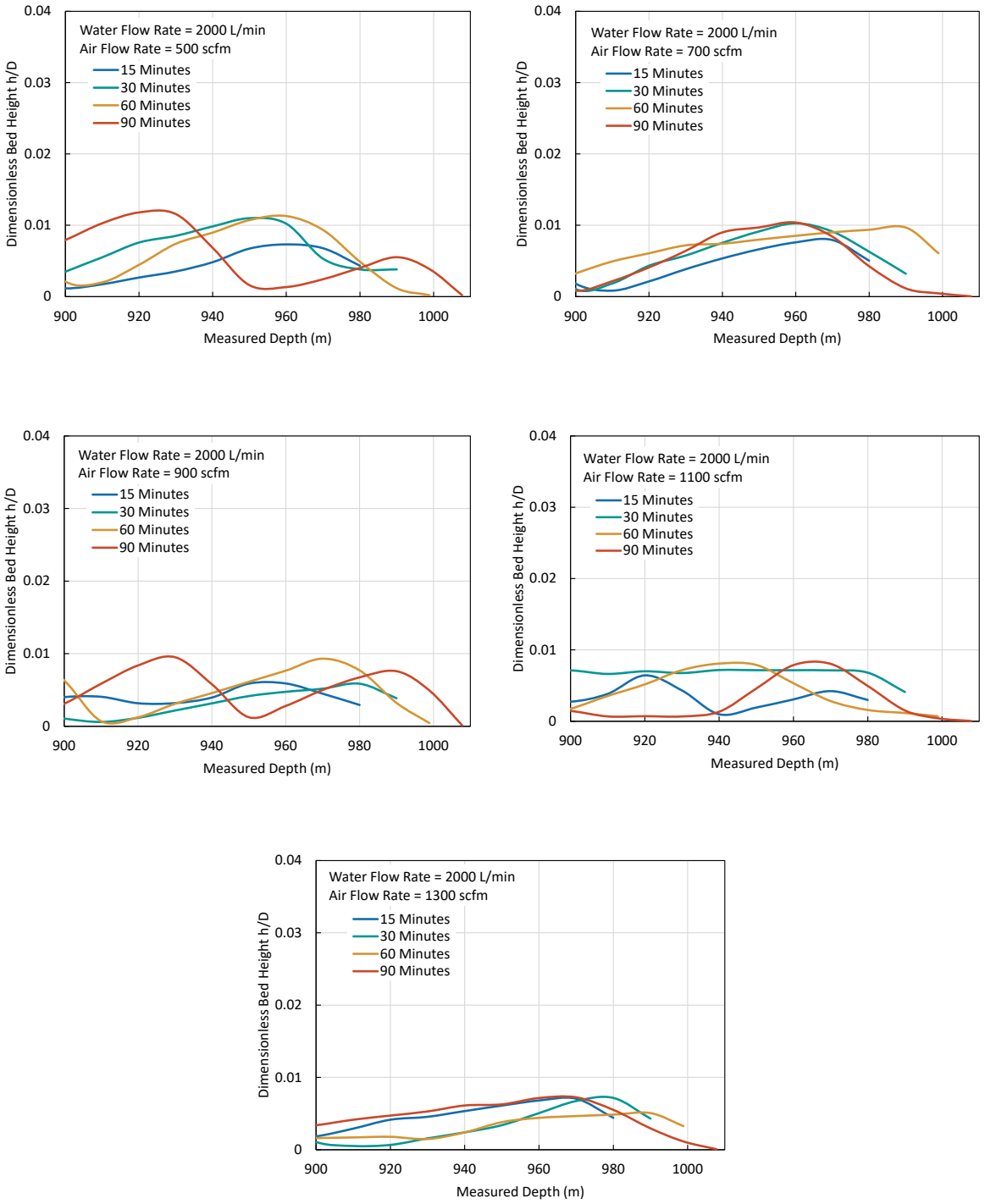

Figure 28: Bed height characteristics for 2000 l/min water with air flow rates 500-1300 scfm.

5.2 Improving Drilling Rate

Figures 16, 19, 21 and 22 show that it is possible to attain higher ROPs and to reduce the total drilling time significantly. Figure 16 from data collected at the rig and Figure 19 show that a

high ROP of up to 20 m/hr could be feasible. The simulation results in Figures 25 to 28 showed that higher ROPs are safe provided that higher water and air flow rates are used. The simulation with flow rates of 1800 l/min of water and 1100 scfm of air showed that the cuttings bed height ratio could be expected to be below 0.01 for that setting.

A combination of different flow rates for water and air showed that high flow rates will significantly improve drilling rate and at the same time effectively transport cuttings to the surface.

From the time depth curve in the Paka field (Figure 8), it can be seen that over time, there has been an improvement in drilling time. This can be attributed to a learning curve due to understanding the field better. Comparing the drilling times for the Olkaria field which ranged from 50 to 60 days to drill to 3000 m (Figure 4), it can be seen that more improvement needs to be made at Paka.

Figure 16 shows that a high ROP of up to 20 m/h could be feasible. Simulation in Figures 25 to 28 showed that a higher ROP of 15 m/h is safe provided that higher water and air flow rates of 1800 l/min and 700 scfm, respectively, are used. Higher pumping rates may enable higher ROPs than 20 m/h but this can also lead to higher costs due to fuel consumption for pumping. A cost benefit analysis will need to be done in order to determine if the higher ROPs that might be feasible with higher pumping is worth the cost.

The cuttings fill characteristics chart as shown in Figure 15 is an indication of ineffective cuttings transportation to the surface. It's also an indication that cuttings transport parameters can be optimized to achieve zero fill of cuttings at the bottom.

The simulated wellbore profile in Figure 18 indicates that the cuttings bed is forming on the inclined side of the well. This result agrees with many similar past research work done. Hence the resultant model can give dependable results. Cuttings beds do not form on the vertical section of the well.

Figure 21 showing the phase velocity profiles indicates that the lowest solid velocity is 0.4 m/s. It is recommended that a minimum solid velocity of 0.25 m/s be achieved in order to effectively transport cuttings to the surface. The velocity shows that there is room for more cuttings to be generated by increasing ROP.

The simulated ECD characteristic in Figure 22 shows that the maximum ECD is expected to be about 850 kg/m^3 for the field conditions. Studies have shown that ECD of as low as 1550 kg/m^3 may fracture some formations (Zhang and Yin, 2017). The aerated water fluid results in

low ECD and the risk of fracturing the formation is low. This implies that more cuttings can be generated by increasing ROP without compromising the integrity of the well.

Chapter 6

Conclusion and Recommendations

From the discussion in section 5.2, on the results of the simulations, it can be seen that there is considerable room for increasing ROP safely. The average ROP from the field data in Figure 16 was about 6 m/h. Simulation results showed that this can be safely increased to 15 m/h. It is recommended that higher ROPs can be applied safely

The pumping rate in the field was seen to be mostly below 1500 l/m as shown in Figure 17. This is a possible cause of downhole problems experienced in the Paka field since the simulation showed that the cuttings bed height ratio is above the optimum ratio of about 0.015 for flow rate below 1500 l/m. It is recommended to increase pumping to 1800 l/min for water and 700 scfm for air flow.

Long circulation times of up to 45 minutes was used in the field before adding each stand of drill pipes. Analysis using the solid phase velocity shows it takes only about 30 minutes for the cuttings to move from the bottom to the surface for the studied 1100 m well section. It is recommended to reduce circulation time to 30 minutes and it will be safe to make the next drill pipe connection. This will allow more time to drill ahead and hence reduce overall drilling time.

The simulation results indicated key areas of improvement to reduce the drilling time. The accuracy of the simulation depends on the accuracy of the field data used in calibrating the model. Automated data acquisition and monitoring systems on the rigs will result in more accurate and versatile data. The data can be used to come up with a very accurate model that will be an important tool in guiding making of technical drilling operations decisions in the field. A good model will lead to improved determination of the best parameters to be used which will in turn lead to improvement in drilling performance. Kenya is currently carrying out drilling campaigns in new geothermal fields which have unique downhole characteristics. It is recommended to simulate the drilling procedure before the actual drilling is conducted in order to give a clear guidance for selecting the operational drilling parameters.

Nomenclature

The symbols used are as follows.

A_1 = cross-sectional annular area of Layer 1, m^2

A_2 = cross-sectional annular area of Layer 2, m^2

C_D = drag coefficient

C_L = lift coefficient

C_{l1} = concentration of liquid phase in Layer l, fraction

C_{l2} = concentration of liquid phase in Layer 2, fraction

C_{s1}= concentration of solid phase in Layer 1, fraction

C_{s2}= concentration of solid phase in Layer 2, fraction

$c_{i\ (i=1,2,3,4)}$ = isothermal compressibility, psi^{-1}

d_p = diameter of cuttings particle, m

D = diameter of wellbore, m

D_p = outer diameter of drill pipe, m

D_1 = equivalent hydraulic diameter of Layer 1, m

D_2 = equivalent hydraulic diameter of Layer 2, m

e = eccentricity of drill pipe (no units); also drill pipe centreline offset from wellbore centreline (m)

f_{tp} = two-phase friction factor

f_{ns} = non-slip friction factor

f_1 = friction factor at pipe wall in Layer 1

f_2 = friction factor at pipe wall in Layer 2

f_i = interfacial-friction coefficient between Layers 1 and 2

F_D = drag force on the cuttings, N

F_g = gravitational force on the cuttings, N

F_L = lift force on the cuttings, N

F_{sf} = multi-particle-drag force per unit length, N/m

g = acceleration due to gravity, m/s^2

h = cuttings bed height, m

K = consistency index of Bingham fluid, Pa·s^n

L_1 = wetted perimeter of Layer 1, m

L_2 = wetted perimeter of Layer 2, m

L_{12} = contact length of Layers 1 and 2, m

m_{ent} = slope (Check Equation 52)

M_w = gas molecular weight

n = flow-behavior index of Bingham model

p = pressure, Pa

P_{pc} = Pseudocritical pressure, psia

P_{pr} = reduced pressure, ratio

q = flow rate

R = universal gas constant

Re_{dep} = particle Reynolds number in cuttings-deposition rate

Re_p = particle Reynolds number

Re_1 = Reynolds number in Layer 1 friction factor

Re_2 = Reynolds number in Layer 2 friction factor

Re_{12} = Reynolds number in Layers 1 and 2 interfacial-friction coefficient

S = distance along wellbore centre, m

t = time, seconds

T = temperature

T_{pc} = pseudocritical temperature, °R

T_{pr} = reduced temperature, ratio

u_{l2} = velocity of liquid phase in Layer 2, m/s

u_{s2} = velocity of solid phase in Layer 2, m/s

u_{l1} = velocity of solid/liquid mixture in Layer 1, m/s

u_{12} = friction velocity at Layer 1 surface, m/s

u_{12}^* = critical friction velocity at Layer 1 surface, m/s

V = gas volume, m^3

v_{dep} = cuttings-deposition rate, m/s

v_{ent} = cuttings-entrainment rate, m/s

v_p = terminal velocity of cuttings particle, m/s

z = gas compressibility factor

γ = shear rate of fluid, l/s

Γ_{dep} = mass transfer rate per unit length (deposition), (kg/s)/m

Γ_{ent} = mass transfer rate per unit length (entrainment), (kg/s)/m

η = dry friction factor

μ_1 = viscosity of solid/liquid mixture in Layer 1, Pa·s^n

ρ_g = density of gas, kg/m^3

ρ_l = density of liquid, kg/m^3

ρ_s = density of solid, kg/m^3

ρ_r = reduced density, ratio

ρ_1 = density of solid/liquid mixture in Layer 1, kg/m^3

τ = shear stress of fluid, N/m^2

τ_1 = shear stress at pipe wall in Layer 1, N/m^2

τ_2 = shear stress at pipe wall in Layer 2, N/m^2

τ_{12} = interfacial shear stress between Layers 1 and 2, N/m^2

τ_y = yield point of Bingham fluid, N/m^2

ϕ = inclination angle of well, rad

References

Azar, J. J. and Samuel, G. R.: *Drilling Engineering*. PennWell Corporation (2007).

Beggs, H. D. and Brill, J. P.: "A study of two-phase flow in inclined pipes." *Journal of Petroleum Technology*, 607–617 (1973).

Bourgoyne, A. T., Millheim, K. K., Chenevert, M. E. and Young, F. S.: *Applied Drilling Engineering*. Society of Petroleum Engineers (1991).

Chien, S. F.: "Annular Velocity for Rotary Drilling Operations." SPE-2786-MS (1969).

Erge, O. and van Oort, E.: "Time-dependent cuttings transport modeling considering the effects of eccentricity, rotation and partial blockage in wellbore annuli." *Journal of Natural Gas Science and Engineering*, **82**, 103488 (2020).

Doan, Q. T. and Oguztoreli, M.: *Numerical Modelling—Critical Flow Rate Determination for Hole Cleaning Calculation in Underbalanced Drilling*, PDVSA/Intevep-JNOC/TRC Collaborative Research Project, The Thermal Hydraulic Aspects of Underbalanced Drilling, Phase II, Task 2a, Final Report (2001).

Dranchuk, P. M. and Abou-Kassem, H.: "Calculation of Z Factors For Natural Gases Using Equations of State." *Journal of Canadian Petroleum Technology*. **14** (3), 34–36 (1975).

Ford, J.: *Drilling Engineering*. Herriot-Watt University, Department of Petroleum Engineering (2004).

GDC: *PW-03B Well Completion Report*. Internal Report of the Geothermal Development Company (GDC), Kenya (2022).

Guo, B. and Liu, G.: *Applied Drilling Circulation Systems: Hydraulics, Calculations, and Models*. Gulf Professional Publishing (2011).

Hall, K. R. and Yarborough, L.: "A new equation-of-state for z-factor calculations." *Oil and Gas Journal,* June 18, 82–92 (1973).

Lee, A. L., Gonzalez, M. H. and Eakin, B. E.: "The viscosity of natural gases." *Journal of Petroleum Technology*, 997–1000 (1966).

Lyons, W. C. and Plisga, G. J.: *Standard Handbook of Petroleum and Natural Gas Engineering*, 2nd Ed., Gulf Professional Publishing (2005).

Macharia, M. W., Gachari, M. K., Kuria, D. N. and Mariita, N. O.: "Low cost geothermal energy indicators and exploration methods in Kenya." *Journal of Geography and Regional Planning*, **10** (9), 254–265 (2017).

Mibei, G., Harðarson, B. S., Franzson, H., Bali, E., Geirsson, H. and Guðfinnsson, G. H.: "Eruptive history and volcano-tectonic evolution of Paka volcanic complex in the Northern Kenya rift: insights into the geothermal heat source." *Journal of African Earth Sciences* **173**, 103951 (2021).

Mibei, G., Harðarson, B. S., Franzson, H., Bali, E., Geirsson, H., Guðfinnsson, G. H., Lichoro, C. and Lagat, J.: "Reservoir characterization of the Paka geothermal system in Kenya: Insights from borehole PK-01." *Geothermics*, **98**, 102293 (2022).

Moore, P. L.: *Drilling Practices Manual*, Petroleum Publishing Company, Tulsa (1974).

Mutonga, M.: "Geothermal geology of Silali volcano in Kenya." *Geothermal Resources Council Transaction*, **36**, 943–949 (2012).

Naganawa, S.: "Experimental study of effective cuttings transport in drilling highly inclined geothermal wells." *Journal of Japanese Association for Petroleum Technology*, **78** (3), 257–264 (2013).

Naganawa, S., Oikawa, A., Masuda, Y., Yonezawa, T., Hoshino, M. and Acuña, P.: "Cuttings transport in directional and horizontal wells while aerated mud drilling." *Proceedings: IADC/SPE Asia Pacific Drilling Technology*, Jakarta, Indonesia. SPE-77195-MS (2002).

Naganawa, S. and Nomura, T.: "Simulating transient behavior of cuttings transport over whole trajectory and of extended reach well." *Proceedings: IADC/SPE Asia Pacific Drilling Technology Conference and Exhibition*. Bangkok, Thailand, SPE-103923-MS (2006).

Naganawa, S. and Okatsu, K.: "Fluctuating of equivalent circulation density in extended reach drilling with repeated formation and erosion of cuttings bed." *Proceedings: IADC/SPE Asia Pacific Drilling Technology Conference and Exhibition*. Jakarta, Indonesia, SPE-115149-MS (2008).

Naganawa, S., Sato, R., and Ishikawa, M.: "Cuttings-transport simulation combined with large-scale-flow-loop experimental results and logging-while-drilling data for hole-cleaning evaluation in directional drilling." *SPE Drilling & Completion*, **32** (3), 194–207 (2017).

Okwiri, L.: “Geothermal drilling time analysis: A case study of Menengai and Hengill.” *Proceedings: World Geothermal Congress*, Melbourne, Australia (2015).

Ong’au, T. M.: *Controlled Directional Drilling in Kenya and Iceland*, Report 20, United Nations University, Geothermal Training Programme, 365–390 (2010).

Ong’au, T. M.: “Controlled directional drilling in Kenya and Iceland (time analysis).” *Geothermal Resources Transaction*, **36**, 177–184 (2012).

Ozbayoglu, M. E., Kuru, E., Stefan, M. and Nicholas, T.: “A comparative study of hydraulic models for foam drilling” *Proceedings: International Conference on Horizontal Well Technology*. Calgary, Alberta, Canada, SPE-65489-MS (2000).

Saleh, F., Teodoriu, C., Salehi, S. and Ezeakacha, C.: “Geothermal drilling: A review of drilling challenges with mud design and lost circulation problem.” *Proceedings: Stanford Geothermal Workshop*, Stanford, California (2020).

Sample, K. J. and Bourgoyne, A. T.: “Development of improved laboratory and field procedures for determining the carrying capacity of drilling fluids.” *Proceedings: SPE Annual Technical Conference and Exhibition*, Houston, Texas, SPE-7497-MS (1978).

Shook, C. A. and Roco, M. C.: *Slurry Flow: Principals and Practice*, Butterworth-Heinemann, Boston, Massachusetts (1991).

Simiyu, S. M.: “Status of geothermal exploration in Kenya and future plans for its development.” *Proceedings: World Geothermal Congress*, Bali, Indonesia, 25–29 (2010).

Standing, M. B. and Katz, D. L.: “Density of Natural Gases.” *Transactions of the AIME*, **146** (1), 140–149, SPE-942140-G (1942).

Terry, R. E., Rogers, J. B. and Craft, B. C.: *Applied Petroleum Reservoir Engineering.* Pearson Education (2015).

Uematsu, H.: *Development of Cuttings Transport Simulator for Deviated Wells*, Master Thesis, University of Tokyo (2003). in Japanese

Walker, R. E. and Mayes, T. M.: “Design of muds for carrying capacity.” *Journal of Petroleum Technology*, **27** (7), 893–900 (1975).

Zhang, J. and Yin, S. X.: “Fracture gradient prediction: An overview and an improved method.” *Petroleum Science*, **14**, 720–730 (2017).